

Absolutely convergent fixed-point fast sweeping WENO methods for steady state of hyperbolic conservation laws

Liang Li¹, Jun Zhu², Yong-Tao Zhang³

Abstract

Fixed-point iterative sweeping methods were developed in the literature to efficiently solve steady state solutions of Hamilton-Jacobi equations and hyperbolic conservation laws. Similar as other fast sweeping schemes, the key components of this class of methods are the Gauss-Seidel iterations and alternating sweeping strategy to achieve fast convergence rate. A family of characteristics of the corresponding hyperbolic partial differential equations (PDEs) are covered in a certain direction simultaneously in each sweeping order. Furthermore, good properties of fixed-point iterative sweeping methods which are different from other fast sweeping methods include that they have explicit forms and do not involve inverse operation of nonlinear local systems, and they can be applied to general hyperbolic equations using any monotone numerical fluxes and high order approximations easily. In a recent article [L. Wu, Y.-T. Zhang, S. Zhang and C.-W. Shu, *Commun. Comput. Phys.*, 20 (2016), 835-869], a fifth order fixed-point sweeping WENO scheme was designed for solving steady state of hyperbolic conservation laws, and it was shown that the scheme converges to steady state solution much faster than the regular total variation diminishing (TVD) Runge-Kutta time-marching approach by stability improvement of high order schemes with a forward Euler time-marching. An open problem is that for some benchmark numerical examples, the iteration residue of the fixed-point sweeping WENO scheme hangs at a truncation error level instead of settling down to machine zero. This issue makes it difficult to determine the convergence criterion for the iteration and challenging to apply the method to complex problems. To solve this issue, in this paper we apply the multi-resolution WENO scheme developed in [J. Zhu and C.-W. Shu, *J. Comput. Phys.*, 375 (2018), 659-683] to the fifth order fixed-point sweeping WENO scheme and obtain an absolutely convergent fixed-point fast sweeping method for steady state of hyperbolic conservation laws, i.e., the residue of the fast sweeping iterations converges to machine zero / round off errors for all benchmark problems tested. Extensive numerical experiments, including solving difficult problems such as the shock reflection and supersonic flow past plates, are performed to show the accuracy, computational efficiency, and absolute convergence of the presented fifth order sweeping scheme.

Key Words: Fixed-point fast sweeping methods, high order accuracy WENO methods, multi-resolution WENO schemes, steady state, hyperbolic conservation laws, convergence.

1 Introduction

Steady state problems for hyperbolic conservation laws and Hamilton-Jacobi equations are common mathematical models appearing in many applications, such as compressible fluid mechanics, optimal control, geometric optics, image processing and computer vision, etc. An essential property of these boundary value problems is that their solution information propagates along characteristics starting from the boundary. For spatial discretization of these hyperbolic type PDEs, weighted

¹ College of Science, Nanjing University of Aeronautics and Astronautics, Nanjing, Jiangsu 210016, P.R. China. E-mail: liliangnuaa@163.com.

² College of Science, Nanjing University of Aeronautics and Astronautics, Nanjing, Jiangsu 210016, P.R. China. E-mail: zhujun@nuaa.edu.cn. Research was supported by NSFC grant 11872210 and Science Challenge Project, No. TZ2016002.

³ Department of Applied and Computational Mathematics and Statistics, University of Notre Dame, Notre Dame, IN 46556, USA. E-mail: yzhang10@nd.edu. Research was partially supported by NSF grant DMS-1620108.

essentially non-oscillatory (WENO) schemes are a popular class of high order accuracy numerical methods. They have the advantage of attaining uniform high order accuracy in smooth regions of the solution while maintaining sharp and essentially non-oscillatory transitions of discontinuities. The first WENO scheme was constructed in [16] for a third-order accurate finite volume version. In [11], third- and fifth-order accurate finite difference WENO schemes in multi-space dimensions were developed, with a general framework for the design of the smoothness indicators and nonlinear weights. To deal with problems defined on complex domain geometries, WENO schemes on unstructured meshes were designed, e.g., see [10, 12, 17, 29, 30]. Recently, WENO schemes on unequal-sized sub-stencils were designed [35, 37], based on the idea in the central WENO schemes [13, 2]. The WENO schemes on unequal-sized sub-stencils exhibit many interesting properties, especially advantages on unstructured meshes and solving steady state problems, see e.g. [38, 39].

After spatial discretization of a steady state problem by a high order WENO scheme, a large nonlinear system is obtained. An important factor which determines computational efficiency for solving steady state problems is the iterative scheme designed for the nonlinear system. For solving a highly coupled nonlinear system resulted from a high order WENO spatial discretization, one choice is to apply the Newton iterations or a more robust method such as the homotopy method [9]. Another efficient approach is to use the fast sweeping iterative method to solve the large nonlinear system. Fast sweeping method is a class of efficient iterative methods which were originally developed to solve static Hamilton-Jacobi equations (see e.g. [33, 18, 19, 7]). Fast sweeping methods utilize alternating sweeping strategy to cover a family of characteristics in a certain direction simultaneously in each sweeping order. Coupled with the Gauss-Seidel iterations, these methods can achieve a fast convergence speed for computations of steady state solutions of hyperbolic PDEs. In [32], fast sweeping methods were first time applied in solving the large nonlinear systems resulted from a WENO spatial discretization, where high order WENO fast sweeping schemes for solving static Hamilton-Jacobi equations were developed. In the WENO fast sweeping methods [32], an explicit strategy in the iterative schemes was designed to avoid directly solving very complicated local nonlinear equations derived from high order WENO discretizations. The methods were combined with accurate boundary treatment techniques in [25]. Fast sweeping techniques were also applied in discontinuous Galerkin (DG) methods to efficiently solve static Hamilton-Jacobi equations, see e.g. [15, 28, 23].

In order to solve steady state problems of other types of hyperbolic PDEs such as the nonlinear hyperbolic conservation laws by high order WENO fast sweeping schemes, the fixed-point sweeping methods were adopted [4, 24]. Fixed-point sweeping WENO methods were first designed in [31] for solving static Hamilton-Jacobi equations. This kind of iterative methods have good properties which are different from other fast sweeping methods include that they have explicit forms and do not involve inverse operation of nonlinear local systems, and they can be applied in solving general hyperbolic equations using any monotone numerical fluxes and high order approximations (e.g. high order WENO approximations) easily. It is interesting to find that although they were developed in different ways, the case of using the Lax-Friedrichs flux in the third order fixed-point sweeping schemes [4] is equivalent to a third order Lax-Friedrichs fast sweeping method to solve steady state problems for hyperbolic conservation laws, which was designed in [5]. In the recent work [24], a fifth order fixed-point sweeping WENO method for efficiently solving steady state problems of hyperbolic conservation laws was developed. Numerical experiments showed that the method converges to steady state solutions much faster than regular time-marching approach, and the acceleration of computation is essentially achieved via using fast sweeping techniques for stability improvement of high order WENO schemes with a forward Euler time-marching to steady state solutions. An open problem in the high order fixed-point sweeping WENO methods such as the fifth order scheme [24] is that for some benchmark numerical examples, the iteration residue of

the fixed-point sweeping WENO scheme hangs at a truncation error level instead of settling down to machine zero / round off errors. This issue makes it difficult to determine the convergence criterion for the iteration and challenging to apply the method to complex problems in real applications. Studies on high order WENO schemes on unequal-sized sub-stencils reveal that they improve the convergence of classical high order WENO schemes to steady state solutions so that the residue of TVD Runge-Kutta iterations settles down to machine zero / round off errors [39]. In this paper, to resolve that open issue in high order fixed-point fast sweeping methods, we apply the fifth order multi-resolution WENO scheme in [37] to the fifth order fixed-point sweeping scheme and obtain an absolutely convergent fixed-point fast sweeping method for steady state of hyperbolic conservation laws, namely, the residue of the fast sweeping iterations converges to machine zero / round off errors for all benchmark problems tested. Extensive numerical experiments, including solving difficult problems such as the shock reflection and supersonic flow past plates, are performed to show the accuracy, computational efficiency, and absolute convergence of the presented fifth order sweeping scheme.

The rest of the paper is organized as follows. The detailed numerical algorithm is described in Section 2. In Section 3 we provide extensive numerical experiments to test and study the proposed method, and to perform comparisons of different methods. Concluding remarks are given in Section 4.

2 Description of the numerical methods

We consider steady state problems of hyperbolic conservation laws with appropriate boundary conditions. The two dimensional (2D) case has the following general form

$$f(u)_x + g(u)_y = R, \quad (2.1)$$

where u is the vector of the unknown conservative variables, $f(u)$ and $g(u)$ are the vectors of flux functions, and $R(u, x, y)$ is the source term. For example, the steady Euler system of equations in compressible fluid dynamics has that $u = (\rho, \rho u, \rho v, E)^T$, $f(u) = (\rho u, \rho u^2 + p, \rho uv, u(E + p))^T$, and $g(u) = (\rho v, \rho uv, \rho v^2 + p, (E + p))^T$. Here ρ is the density of fluid, $(u, v)^T$ is the velocity vector, p is the pressure, and $E = \frac{p}{\gamma' - 1} + \frac{1}{2}\rho(u^2 + v^2)$ is total energy where the constant $\gamma' = 1.4$ for the case of air. A spatial discretization of (2.1) by a high order WENO scheme leads to a large nonlinear system of algebraic equations with the size determined by the number of spatial grid points.

2.1 The fifth order multi-resolution WENO discretization

WENO schemes with unequal-sized sub-stencils [35, 39] have shown nice property in convergence to steady states. In this paper, we adopt the fifth order multi-resolution WENO scheme [37] for the spatial discretization of (2.1) in order to achieve an absolutely convergent fixed-point fast sweeping method for steady state of hyperbolic conservation laws.

For the flux terms $f(u)_x + g(u)_y$, the conservative finite difference scheme is used to approximate them at a grid point (x_i, y_j) of a uniform (or smoothly varying) mesh

$$(f(u)_x + g(u)_y)|_{x=x_i, y=y_j} \approx \frac{1}{\Delta x}(\hat{f}_{i+1/2, j} - \hat{f}_{i-1/2, j}) + \frac{1}{\Delta y}(\hat{g}_{i, j+1/2} - \hat{g}_{i, j-1/2}), \quad (2.2)$$

where $\hat{f}_{i+1/2, j}$ and $\hat{g}_{i, j+1/2}$ are the numerical fluxes, and $\Delta x, \Delta y$ are grid sizes of x, y directions respectively. In the following we describe the detailed procedure for reconstructing the numerical flux $\hat{f}_{i+1/2, j}$ in the x direction. Similar procedure is applied to the y direction for $\hat{g}_{i, j+1/2}$.

For upwinding and linear stability of the scheme, we perform a splitting of the flux $f(u)$, i.e., $f(u) = f^+(u) + f^-(u)$, which satisfies the condition that $\frac{df^+(u)}{du} \geq 0$ and $\frac{df^-(u)}{du} \leq 0$ for the scalar case, or the corresponding eigenvalues of that Jacobian matrix are positive / negative for the system case with a local characteristic decomposition. A simple Lax-Friedrichs flux splitting $f^\pm(u) = \frac{1}{2}(f(u) \pm \alpha u)$ is used here, where $\alpha = \max_u |f'(u)|$. Then each of them is approximated separately by the WENO scheme using different stencils to find numerical fluxes $\hat{f}_{i+1/2,j}^+$ and $\hat{f}_{i+1/2,j}^-$ respectively. The final numerical flux is $\hat{f}_{i+1/2,j} = \hat{f}_{i+1/2,j}^+ + \hat{f}_{i+1/2,j}^-$.

To reconstruct $\hat{f}_{i+1/2,j}^+$ along the line $y = y_j$, we first identify the numerical values $f^+(u_{l,j})$ to be cell averages of a function $h(x)$ on cell $I_l = [x_{l-1/2}, x_{l+1/2}]$ of the x-direction, for all l . Here $x_{l+1/2} = (x_l + x_{l+1})/2$, and $u_{l,j}$ denotes the numerical solution of u at the grid point (x_l, y_j) . Then, with the information of cell averages

$$f^+(u_{l,j}) = \bar{h}_l = \frac{1}{\Delta x} \int_{x_{l-1/2}}^{x_{l+1/2}} h(x) dx,$$

the following reconstruction algorithm is performed.

Reconstruction algorithm:

Step 1. We choose the central spatial stencils $T_k = \{I_{i+1-k}, \dots, I_{i-1+k}\}$, $k = 1, 2, 3$, and reconstruct $2k - 2$ degree polynomials $q_k(x)$ which satisfy

$$\frac{1}{\Delta x} \int_{x_{l-1/2}}^{x_{l+1/2}} q_k(x) dx = \bar{h}_l, l = i - k + 1, \dots, i - 1 + k; k = 1, 2, 3.$$

Step 2. Obtain equivalent expressions for these reconstruction polynomials of different degrees. To keep consistent notation, we denote $p_1(x) = q_1(x)$, with similar ideas for the central WENO schemes [13, 2, 14] as well, and compute

$$p_2(x) = \frac{1}{\gamma_{2,2}} q_2(x) - \frac{\gamma_{1,2}}{\gamma_{2,2}} p_1(x),$$

$$p_3(x) = \frac{1}{\gamma_{3,3}} q_3(x) - \frac{\gamma_{1,3}}{\gamma_{3,3}} p_1(x) - \frac{\gamma_{2,3}}{\gamma_{3,3}} p_2(x),$$

with $\gamma_{1,2} + \gamma_{2,2} = 1$, $\gamma_{1,3} + \gamma_{2,3} + \gamma_{3,3} = 1$, and $\gamma_{2,2} \neq 0, \gamma_{3,3} \neq 0$. In these expressions, $\gamma_{a,b}$ for $a = 1, \dots, b$ and $b = 2, 3$ are the linear weights. Based on a balance between the sharp and essentially non-oscillatory shock transitions in nonsmooth regions and accuracy in smooth regions, following the practice in [6, 34, 17, 35, 37], we take the linear weights as $\gamma_{1,2} = \frac{1}{11}$, $\gamma_{2,2} = \frac{10}{11}$, $\gamma_{1,3} = \frac{1}{111}$, $\gamma_{2,3} = \frac{10}{111}$, $\gamma_{3,3} = \frac{100}{111}$.

Step 3. Compute the smoothness indicators β_k , which measure how smooth the functions $p_k(x)$ for $k = 2, 3$ are in the interval $[x_{i-1/2}, x_{i+1/2}]$. We use the same recipe for the smoothness indicators as that in [11, 21]:

$$\beta_k = \sum_{\alpha=1}^{2k-2} \int_{x_{i-1/2}}^{x_{i+1/2}} \Delta x^{2\alpha-1} \left(\frac{d^\alpha p_k(x)}{dx^\alpha} \right)^2 dx, \quad k = 2, 3.$$

The only exception is β_1 , which is magnified from zero to a tiny value. See [37] for details.

Step 4. Compute the nonlinear weights based on the linear weights and the smoothness indicators. We adopt the WENO-Z type nonlinear weights as that in [1, 3]. First a quantity τ

which depends on the absolute differences between the smoothness indicators is calculated: $\tau = \left(\frac{\sum_{l_1=1}^2 |\beta_3 - \beta_{l_1}|}{2}\right)^2$. The nonlinear weights are then computed as

$$\omega_{l_1} = \frac{\bar{\omega}_{l_1}}{\sum_{l_2=1}^3 \bar{\omega}_{l_2}}, \quad \bar{\omega}_{l_1} = \gamma_{l_1,3} \left(1 + \frac{\tau}{\varepsilon + \beta_{l_1}}\right), \quad l_1 = 1, 2, 3.$$

ε is a small value to avoid that the denominator becomes zero. In this paper, ε is taken to be 10^{-6} for all numerical examples.

Step 5. The final reconstructed numerical flux $\hat{f}_{i+1/2,j}^+$ is given by

$$\hat{f}_{i+1/2,j}^+ = \sum_{l_1=1}^3 \omega_{l_1} p_{l_1}(x_{i+1/2}).$$

The reconstruction of the numerical flux $\hat{f}_{i+1/2,j}^-$ is mirror-symmetric with respect to $x_{i+1/2}$.

2.2 Absolutely convergent fixed-point sweeping WENO scheme

After the spatial discretization of the PDE (2.1) by a WENO scheme with unequal-sized sub-stencils such as the fifth order multi-resolution WENO scheme described in the last section, we obtain a nonlinear algebraic system

$$0 = -(\hat{f}_{i+1/2,j} - \hat{f}_{i-1/2,j})/\Delta x - (\hat{g}_{i,j+1/2} - \hat{g}_{i,j-1/2})/\Delta y + R(u_{ij}, x_i, y_j), \quad i = 1, \dots, N; j = 1, \dots, M, \quad (2.3)$$

where N, M are the number of grid points in the x and y directions respectively.

The fixed-point fast sweeping schemes for solving the nonlinear system (2.3) are based on iterative schemes of time marching type for solving steady state problems. Time marching approach for solving steady state problems is essentially a Jacobi type fixed-point iterative scheme. The right-hand-side (RHS) of (2.3) is a nonlinear function of numerical values at the grid points of computational stencils. We denote it by L . The forward Euler (FE) time marching method with time step size $\Delta t_n = \frac{\gamma}{\alpha_x/\Delta x + \alpha_y/\Delta y}$ is actually the following Jacobi type fixed-point iterative scheme

$$u_{ij}^{n+1} = u_{ij}^n + \frac{\gamma}{\alpha_x/\Delta x + \alpha_y/\Delta y} L(u_{i-r,j}^n, \dots, u_{i+s,j}^n; u_{ij}^n; u_{i,j-r}^n, \dots, u_{i,j+s}^n),$$

$$i = 1, \dots, N; j = 1, \dots, M; \quad (2.4)$$

where r, s are values which depend on the order of the WENO reconstruction. For the fifth order multi-resolution WENO scheme used here, we have $r = s = 3$. n denotes the iteration step. The values $\alpha_x = \max_u |f'(u)|$ and $\alpha_y = \max_u |g'(u)|$ for the scalar equations, or they are the maximum absolute values of eigenvalues of the Jacobian matrices $f'(u)$ and $g'(u)$ for the system cases. Actually α_x and α_y represent the maximum characteristic speeds in each spatial direction, and they are updated in every iteration. γ is a parameter. To guarantee that the fixed-point iteration is a contractive mapping and converges, suitable values of γ need to be chosen. In the context of time marching methods, γ is actually the Courant-Friedrichs-Lewy (CFL) number. Because accuracy of the scheme in the time discretization does not affect the final results of solutions of steady state problems, it sounds good that the FE time marching method is a better choice than high order time schemes such as Runge-Kutta (RK) schemes since its simplicity with only single step and

single stage involved. However, high order linear schemes which are the building blocks for high order spatial discretization schemes such as WENO schemes, has linear stability issues when they are marched by the forward Euler time discretization to solve hyperbolic PDEs. Even with the help of a nonlinearly stable discretization such as a WENO scheme, the Jacobi fixed-point iterative scheme (2.4) still needs many iteration steps to converge [24].

One way to resolve this issue is to use high order TVD RK schemes [22, 8], which can maintain both linear and nonlinear stability when they are coupled with high order nonlinearly stable spatial discretizations. Similar as the FE time marching, RK time marching methods are also Jacobi type fixed-point iterations. For example, the popular third order TVD RK (TVD RK3) scheme [22] can be written as the following Jacobi type fixed-point iteration scheme for solving the nonlinear system (2.3):

$$u_{ij}^{(1)} = u_{ij}^n + \frac{\gamma}{\alpha_x/\Delta x + \alpha_y/\Delta y} L(u_{i-r,j}^n, \dots, u_{i+s,j}^n; u_{i,j}^n; u_{i,j-r}^n, \dots, u_{i,j+s}^n),$$

$$i = 1, \dots, N; j = 1, \dots, M, \quad (2.5)$$

$$u_{ij}^{(2)} = \frac{3}{4}u_{ij}^n + \frac{1}{4}u_{ij}^{(1)} + \frac{\gamma}{4(\alpha_x/\Delta x + \alpha_y/\Delta y)} L(u_{i-r,j}^{(1)}, \dots, u_{i+s,j}^{(1)}; u_{i,j}^{(1)}; u_{i,j-r}^{(1)}, \dots, u_{i,j+s}^{(1)}),$$

$$i = 1, \dots, N; j = 1, \dots, M, \quad (2.6)$$

$$u_{ij}^{n+1} = \frac{1}{3}u_{ij}^n + \frac{2}{3}u_{ij}^{(2)} + \frac{2\gamma}{3(\alpha_x/\Delta x + \alpha_y/\Delta y)} L(u_{i-r,j}^{(2)}, \dots, u_{i+s,j}^{(2)}; u_{i,j}^{(2)}; u_{i,j-r}^{(2)}, \dots, u_{i,j+s}^{(2)}),$$

$$i = 1, \dots, N; j = 1, \dots, M. \quad (2.7)$$

Although the TVD RK3 scheme (2.5)-(2.7) involves three stages in one time step, it can permit a much larger γ than the FE scheme (2.4) in order to ensure that the fixed-point iterations converge, hence much less iterations are needed as that shown in [24] and also the next section of this paper. It is a popular method to march numerical solutions of high order WENO schemes to steady states, see e.g. [11, 39].

In order to achieve faster convergence to steady state solutions of high order WENO schemes for solving hyperbolic PDEs than the Jacobi type fixed-point iterations, one approach is to apply the fast sweeping techniques so that the important characteristics property of hyperbolic PDEs can be utilized in the iterations. As shown in the numerical experiments of [24] and this paper, by applying the fast sweeping techniques to the fixed-point schemes, we can obtain much more efficient iterative schemes. Especially for the FE scheme, the number of iteration steps to the steady state is reduced significantly and the CFL number γ is much larger than that in the Jacobi iterations. In fact, after applying the fast sweeping techniques, the FE scheme can have a comparable CFL number γ as that of the TVD RK3 scheme, and it is more efficient than the TVD RK3 scheme to reach steady state of the solutions.

The fast sweeping methods have two essential components, i.e., the Gauss-Seidel philosophy and alternating direction iterations. The Gauss-Seidel philosophy requires that the newest numerical values of u are used in the fifth order multi-resolution WENO reconstruction stencils as long as they are available. With the fifth order multi-resolution WENO reconstruction described in the last section, we form an absolutely convergent fixed-point fast sweeping method. The residue of the new fixed-point fast sweeping iterations converges to machine zero / round off errors for all

benchmark problems tested in the next section. The form of this FE type fixed-point fast sweeping scheme is:

$$u_{ij}^{n+1} = u_{ij}^n + \frac{\gamma}{\alpha_x/\Delta x + \alpha_y/\Delta y} L(u_{i-r,j}^*, \dots, u_{i+s,j}^*; u_{i,j}^n; u_{i,j-r}^*, \dots, u_{i,j+s}^*),$$

$$i = i_1, \dots, i_N; j = j_1, \dots, j_M. \quad (2.8)$$

Here the operator L denotes the fifth order multi-resolution WENO spatial discretization. The iteration direction that is marked as “ $i = i_1, \dots, i_N; j = j_1, \dots, j_M$ ” means that the iterations in the scheme (2.8) do not just proceed in only one direction $i = 1 : N, j = 1 : M$ as that in the Jacobi type schemes, but in the following four alternating directions repeatedly,

- (1) $i = 1 : N, j = 1 : M;$
- (2) $i = N : 1, j = 1 : M;$
- (3) $i = N : 1, j = M : 1;$
- (4) $i = 1 : N, j = M : 1.$

Since the strategy of alternating direction sweepings utilizes the characteristics property of hyperbolic PDEs, combining with the Gauss-Seidel philosophy, we are able to observe the acceleration of convergence speed, which will be shown in the following numerical experiments. By the Gauss-Seidel philosophy, we use the newest numerical values on the computational stencil of the WENO scheme whenever they are available. That is the reason we use the notation u^* to represent the values in the scheme (2.8), and $u_{k,l}^*$ could be $u_{k,l}^n$ or $u_{k,l}^{n+1}$, depending on the current sweeping direction.

Remark 1. The fast sweeping techniques can also be applied to the TVD RK3 scheme (2.5)-(2.7) as that in [24]. However, it was found in [24] that the scheme resulted by applying fast sweeping method to the TVD RK3 scheme (2.5)-(2.7) is less efficient than the FE fast sweeping method. Hence in this paper we only focus on the FE fast sweeping method coupled with the fifth order multi-resolution WENO reconstruction, i.e., the scheme (2.8). Also we emphasize that the scheme (2.8), the FE fast sweeping method coupled with the fifth order multi-resolution WENO reconstruction, is a novel method which is different from the method in our previous work [24]. It improves the previous scheme in [24] by achieving the absolute convergence in the fixed-point fast sweeping iterations to reach steady state of hyperbolic conservation laws, i.e., the residue of the fast sweeping iterations converges to machine zero / round off errors.

Remark 2. It is interesting to see that in the fast sweeping scheme (2.8), during the iteration process the fifth order multi-resolution WENO reconstructions for numerical fluxes at the cell interfaces need to be performed individually for grid points sharing the same cell interface, due to the Gauss-Seidel philosophy. For example, the newest numerical values at the WENO reconstruction stencil for computing the numerical flux $\hat{f}_{i+1/2,j}$ are different when we update the numerical values $u_{i,j}$ and $u_{i+1,j}$. Since the Gauss-Seidel philosophy in the fast sweeping scheme requires that the newest numerical values are always used whenever they are available, the numerical flux $\hat{f}_{i+1/2,j}$ needs to be computed separately for updating $u_{i,j}$ and $u_{i+1,j}$ during the fast sweeping iterations. This is different from the Jacobi iterations. So during the iteration process, the fast sweeping scheme does *not* preserve the conservation. However, this does *not* affect the conservation of the final results at all, because once the fast sweeping iterations converge, the new and old values

converge to the same value, hence numerical fluxes $\hat{f}_{i+1/2,j}$ which are computed separately for $u_{i,j}$ and $u_{i+1,j}$ also converge to the same value. Then the final conservative system (2.3) is resolved and the conservation of the final results is preserved. Also from the numerical experiments shown in the next section, the fast sweeping iterations are much more efficient than the Jacobi type time marching iterations.

3 Numerical experiments

In this section we perform numerical experiments to test the performance of the proposed fifth order absolutely convergent fixed-point fast sweeping WENO scheme for solving steady-state problems. These numerical examples come from the literature about numerical studies on steady state solutions of hyperbolic conservation laws, e.g., [24, 36, 39]. Computational efficiency of the fast sweeping scheme and the other two iterative schemes discussed in the last section is compared. For the convenience of presentation, we name the absolutely convergent fixed-point fast sweeping WENO scheme (2.8) “FE fast sweeping scheme”, the forward Euler time marching scheme (2.4) “FE Jacobi scheme”, the popular TVD RK3 time marching scheme (2.5)-(2.7) “RK Jacobi scheme”. We perform mesh refinement study and calculate L_1 and L_∞ numerical errors and accuracy orders of these iterative schemes. Iteration numbers and CPU times of each iterative scheme to converge are recorded for comparison of their efficiency. The convergence of the iterations is measured by the average residue defined as

$$ResA = \sum_{i=1}^{\mathcal{N}} \frac{|R_i|}{\mathcal{N}}. \quad (3.1)$$

Here R_i is the local residue at the grid point i and it is defined as

$$R_i = \frac{u_i^{n+1} - u_i^n}{\Delta t_n}.$$

\mathcal{N} is the total number of grid points and n is the iteration step. $\Delta t_n = \frac{\gamma}{\alpha_x/\Delta x + \alpha_y/\Delta y}$. For a system of equations, the average residue $ResA$ is calculated based on the mean of all components of the system. For example, a 2D Euler system has four equations with four conservative variables, so the average residue is defined as $ResA = \sum_{i=1}^{\mathcal{N}} \frac{|R1_i| + |R2_i| + |R3_i| + |R4_i|}{4\mathcal{N}}$ where the $R*_i$'s are the local residuals of different conservative variables, i.e., $R1_i = \frac{\rho_i^{n+1} - \rho_i^n}{\Delta t_n}$, $R2_i = \frac{(\rho u)_i^{n+1} - (\rho u)_i^n}{\Delta t_n}$, $R3_i = \frac{(\rho v)_i^{n+1} - (\rho v)_i^n}{\Delta t_n}$, $R4_i = \frac{E_i^{n+1} - E_i^n}{\Delta t_n}$. The convergence criterion for most examples is set to be $ResA < 10^{-12}$ except that in some examples we use an even smaller threshold value to study the levels that the residues can reach. In this paper, the number of iterations reported in the numerical simulations counts a complete update of numerical values in all grid points once as one iteration.

3.1 Examples with smooth solutions

We first test these schemes using problems with smooth solutions.

Example 1. A 1D Burgers' equation

We compute the steady state solution of the following 1D Burgers' equation with a source term

$$u_t + \left(\frac{u^2}{2}\right)_x = \sin(x) \cos(x), \quad x \in \left[\frac{1}{4}\pi, \frac{3}{4}\pi\right].$$

The initial condition $u(x, 0) = \beta \sin(x)$ is used as the initial guess in the iterations. At the left boundary $x = (1/4)\pi$, an inflow boundary condition is imposed with $u((1/4)\pi, t) = \sqrt{2}/2$. The outflow boundary condition is applied at the right boundary $x = (3/4)\pi$. If $\beta > 1$, the problem has the unique steady state solution $u(x, \infty) = \sin(x)$. We take $\beta = 2$ and use these three different iterative schemes based on the fifth order multi-resolution WENO spatial discretization to compute the steady state solution. For the outflow boundary point $x = (3/4)\pi$ itself and the associated ghost points to the right of $x = (3/4)\pi$ in the stencil of the WENO scheme, extrapolation by a degree 4 polynomial is used to compute numerical values at them. In this example we use $ResA < 10^{-13}$ as the iteration convergence criterion.

The results of numerical accuracy, iteration numbers and CPU costs for three different iterative schemes are presented in Table 1. It is observed that all schemes achieve comparable numerical errors and the fifth order accuracy when the iterations converge. Comparing the algorithm efficiency to reach the steady state, the FE Jacobi scheme (2.4) requires a very small CFL number $\gamma = 0.1$ to have the iterations converge. The reason is that a forward Euler time discretization with a high order linear upwind spatial discretization suffers from linear stability issue. When the nonlinearly stable WENO discretization is applied, it alleviates the linear instability problem. As a result of balance, the FE Jacobi scheme converges under a tiny CFL number. That leads to the largest iteration numbers and the most CPU time among these three iterative schemes. By using a high order TVD RK scheme, for example the TVD RK3, the RK Jacobi scheme (2.5)-(2.7) with a high order WENO discretization is both linearly and nonlinearly stable. Hence here a much larger CFL number $\gamma = 1.0$ can be used to make the iterations converge. We can see that both the iteration numbers and CPU costs are reduced a lot by using the RK Jacobi scheme rather than the FE Jacobi scheme. From Table 1, it can be seen that fast sweeping techniques accelerate the convergence to the steady state significantly. Furthermore, it is important to notice that the FE fast sweeping scheme can have a CFL number $\gamma = 1.0$ which is the same as the TVD RK3 scheme. This shows that the fast sweeping technique improves the linear stability of the forward Euler scheme when it is coupled with a high order spatial discretization. Since the time accuracy does not contribute to the accuracy of a steady state solution, the forward Euler time marching should be preferred because of its simplicity comparing to multi-stage Runge-Kutta schemes. However, due to the linear stability issue when it is coupled with a high order spatial discretization, the forward Euler scheme is not practically useful. Here we can see that this issue is resolved by applying the fast sweeping technique, namely, using the FE fast sweeping scheme rather than the FE Jacobi scheme. Actually, as shown in Tables 1 about the iteration numbers and CPU times, the FE fast sweeping scheme is the most efficient one among all three schemes.

Example 2. A 1D shallow water equation

In this example, we use these iterative schemes to solve a one-dimensional shallow water equation

$$\begin{pmatrix} h \\ hu \end{pmatrix}_t + \begin{pmatrix} hu \\ hu^2 + \frac{1}{2}gh^2 \end{pmatrix}_x = \begin{pmatrix} 0 \\ -ghb_x \end{pmatrix},$$

where h denotes the water height, u is the velocity of the water, $b(x)$ represents the bottom topography, and g is the gravitational constant. The bottom topography is smooth and given by the function

$$b(x) = 5e^{-\frac{2}{5}(x-5)^2}, x \in [0, 10].$$

The steady state solution of the problem is

$$h + b = 10, \quad hu = 0.$$

FE Jacobi, $\gamma=0.1$						
N	L_1 error	L_1 order	L_∞ error	L_∞ order	iter#	CPU time
10	6.27E-07	-	1.54E-06	-	1153	2.0E-02
20	1.93E-08	5.02	8.07E-08	4.25	1458	5.5E-02
40	8.91E-10	4.44	3.21E-09	4.65	1749	0.14
80	3.32E-11	4.75	1.11E-10	4.85	2310	0.30
160	1.13E-12	4.87	3.66E-12	4.92	3875	0.98
320	4.98E-14	4.51	1.70E-13	4.43	7196	3.63
RK Jacobi, $\gamma=1.0$						
N	L_1 error	L_1 order	L_∞ error	L_∞ order	iter#	CPU time
10	8.11E-07	-	3.15E-06	-	285	2.0E-03
20	2.29E-08	5.15	1.19E-07	4.73	330	8.0E-03
40	9.49E-10	4.59	4.00E-09	4.89	429	1.6E-02
80	3.41E-11	4.80	1.29E-10	4.95	630	6.6E-02
160	1.15E-12	4.89	4.35E-12	4.90	1137	0.19
320	4.10E-14	4.81	1.55E-13	4.81	1953	0.58
FE fast sweeping, $\gamma=1.0$						
N	L_1 error	L_1 order	L_∞ error	L_∞ order	iter#	CPU time
10	6.27E-07	-	1.54E-06	-	130	2.0E-03
20	1.93E-08	5.02	8.07E-08	4.25	142	4.0E-03
40	8.91E-10	4.44	3.21E-09	4.65	155	1.1E-02
80	3.32E-11	4.75	1.11E-10	4.85	210	2.9E-02
160	1.12E-12	4.89	3.64E-12	4.93	328	9.7E-02
320	3.64E-14	4.95	1.22E-13	4.90	550	0.28

Table 1: Example 1, A 1D Burgers' equation. Accuracy, iteration numbers and CPU times of three different iterative schemes. CPU time unit: second

FE Jacobi, $\gamma=0.1$						
N	L_1 error	L_1 order	L_∞ error	L_∞ order	iter#	CPU time
20	3.53E-03	-	2.12E-02	-	5676	0.14
40	9.31E-05	5.25	1.37E-03	3.95	4512	0.20
80	1.58E-06	5.88	3.45E-05	5.31	7314	0.66
160	1.59E-08	6.63	4.54E-07	6.25	13023	2.32
320	-	-	-	-	not conv.	-

RK Jacobi, $\gamma=1.0$						
N	L_1 error	L_1 order	L_∞ error	L_∞ order	iter#	CPU time
20	3.53E-03	-	2.12E-02	-	321	2.4E-02
40	9.31E-05	5.25	1.37E-03	3.95	459	6.4E-02
80	1.58E-06	5.88	3.45E-05	5.31	741	0.22
160	1.59E-08	6.63	4.54E-07	6.25	1161	0.62
320	2.02E-10	6.30	6.83E-09	6.05	1734	1.86

FE fast sweeping, $\gamma=1.0$						
N	L_1 error	L_1 order	L_∞ error	L_∞ order	iter#	CPU time
20	3.53E-03	-	2.12E-02	-	221	1.3E-02
40	9.31E-05	5.25	1.37E-03	3.95	121	1.7E-02
80	1.58E-06	5.88	3.45E-05	5.31	144	4.2E-02
160	1.59E-08	6.63	4.54E-07	6.25	228	0.13
320	2.03E-10	6.30	6.83E-09	6.05	379	0.42

Table 2: Example 2, A 1D shallow water equation. Accuracy, iteration numbers and CPU times of three different iterative schemes. CPU time unit: second

To test these iterative schemes, we use the exact solution as the initial guess in the iterations. Because the exact steady state solution of the PDE itself is not the numerical steady states of the schemes, the convergence behavior of iterative schemes starting from it can be observed. We use the exact solution to impose the numerical values at boundary points. The simulation results of these three iterative schemes are reported in Table 2. It can be seen that these schemes give similar numerical errors and higher than fifth order accuracy when the mesh is refined. We observe similar convergence behavior of these three different iterative schemes as that in Example 1, except that in this example, residues of the FE Jacobi scheme with $N = 320$ stop at the level of 10^{-9} and fail to reach the convergence criterion $ResA < 10^{-12}$, even using a very small CFL number $\gamma = 0.1$. Large number of iterations and the most CPU time among three iterative schemes are needed for the FE Jacobi scheme to converge. On the other hand, the FE fast sweeping scheme can use a much larger CFL number $\gamma = 1.0$ and converges with much smaller iteration numbers and CPU times, including the case with the most refined mesh $N = 320$ without any difficulty. Consistent with Example 1, the FE fast sweeping scheme is more efficient than the TVD RK3 (RK Jacobi) scheme and it turns out to be the most efficient scheme among these three iterative schemes. Specifically, CPU times of the FE fast sweeping scheme is about 20% of that of the RK Jacobi scheme on refined meshes.

Example 3. A 2D Burgers' equation

We use the iterative schemes to solve the steady state problem of a two-dimensional Burgers' equation with a source term

$$u_t + \left(\frac{1}{\sqrt{2}} \frac{u^2}{2}\right)_x + \left(\frac{1}{\sqrt{2}} \frac{u^2}{2}\right)_y = \sin\left(\frac{x+y}{\sqrt{2}}\right) \cos\left(\frac{x+y}{\sqrt{2}}\right),$$

$$(x, y) \in \left[\frac{\pi}{4\sqrt{2}}, \frac{3\pi}{4\sqrt{2}}\right] \times \left[\frac{\pi}{4\sqrt{2}}, \frac{3\pi}{4\sqrt{2}}\right].$$

The initial condition

$$u(x, y, 0) = \beta \sin\left(\frac{x+y}{\sqrt{2}}\right)$$

is used as the initial guess in the iterations, and the value of β is taken as 1.5. The exact steady state solution of the problem is

$$u(x, y, \infty) = \sin\left(\frac{x+y}{\sqrt{2}}\right)$$

and it is imposed on boundary points for the purpose of testing these three iterative schemes. $ResA < 10^{-13}$ is used as the iteration convergence criterion. The results for three different iterative schemes are reported in Table 3. Similar as the 1D examples, all three schemes achieve comparable numerical errors and the fifth order accuracy when they converge. However the FE Jacobi scheme requires a very small CFL number to achieve the convergence, hence much more iterations and CPU times than the other two schemes are needed to reach the steady state. The FE fast sweeping scheme is the most efficient one among all three iterative methods as shown in Table 3. We can see that CPU times which are needed by the FE fast sweeping scheme is only about 35% of that of the RK Jacobi (TVD RK3) scheme on the most refined mesh.

Example 4. A 2D Euler system of equations with source terms

FE Jacobi, $\gamma=0.1$						
$N \times N$	L ₁ error	L ₁ order	L _∞ error	L _∞ order	iter#	CPU time
10 × 10	1.47E-08	-	8.60E-08	-	1054	0.31
20 × 20	6.14E-10	4.58	3.28E-09	4.71	1317	1.53
40 × 40	2.22E-11	4.79	1.24E-10	4.73	1850	8.88
RK Jacobi, $\gamma=1.0$						
$N \times N$	L ₁ error	L ₁ order	L _∞ error	L _∞ order	iter#	CPU time
10 × 10	1.81E-08	-	1.43E-07	-	279	9.4E-02
20 × 20	6.87E-10	4.72	5.12E-09	4.80	348	0.42
40 × 40	2.35E-11	4.87	1.64E-10	4.96	519	2.48
FE fast sweeping, $\gamma=1.0$						
$N \times N$	L ₁ error	L ₁ order	L _∞ error	L _∞ order	iter#	CPU time
10 × 10	1.81E-08	-	1.43E-07	-	120	3.3E-02
20 × 20	6.87E-10	4.72	5.12E-09	4.80	137	0.18
40 × 40	2.35E-11	4.87	1.71E-10	4.91	182	0.88

Table 3: Example 3, A 2D Burgers' equation. Accuracy, iteration numbers and CPU times of three different iterative schemes. CPU time unit: second

In this example, we solve the following two-dimensional Euler system of equations with source terms:

$$\frac{\partial}{\partial t} \begin{pmatrix} \rho \\ \rho u \\ \rho v \\ E \end{pmatrix} + \frac{\partial}{\partial x} \begin{pmatrix} \rho u \\ \rho u^2 + p \\ \rho uv \\ u(E + p) \end{pmatrix} + \frac{\partial}{\partial y} \begin{pmatrix} \rho v \\ \rho uv \\ \rho v^2 + p \\ v(E + p) \end{pmatrix} = \begin{pmatrix} 0.4 \cos(x+y) \\ 0.6 \cos(x+y) \\ 0.6 \cos(x+y) \\ 1.8 \cos(x+y) \end{pmatrix}.$$

The exact steady-state solutions of the system are $\rho(x, y, \infty) = 1 + 0.2 \sin(x + y)$, $u(x, y, \infty) = 1$, $v(x, y, \infty) = 1$, and $p(x, y, \infty) = 1 + 0.2 \sin(x + y)$. The computational domain is $(x, y) \in [0, 2\pi] \times [0, 2\pi]$, and we apply the exact steady-state solutions on the domain boundaries. To start the iterations for the schemes, we take the numerical initial conditions to be the same as the exact steady-state solutions, which does not satisfy the numerical schemes and will be driven by the iterative schemes to the numerical steady states. In Table 4, we report the numerical accuracy for the density variable ρ , iteration numbers and CPU times when these three different iterative schemes reach the average residue threshold value 10^{-12} of the convergence criterion. It can be observed that all schemes achieve similar numerical errors and the fifth order accuracy when the iterations converge. Comparing these iterative schemes' efficiency, we obtain the same conclusion as that for the previous problems. The FE Jacobi scheme needs to use a very small CFL number to reach convergence and that leads to large number of iterations and the most CPU time cost among all three schemes, while the FE fast sweeping scheme is the most efficient one among them. We can see that the FE fast sweeping scheme saves more than 50% CPU time cost of that of the RK Jacobi (TVD RK3) scheme. In Figure 1, the convergence history of the residue (3.1) as a function of number of iterations for the FE Jacobi scheme, the RK Jacobi scheme and the FE fast sweeping scheme on different meshes is shown. We can see that the residue settles down to tiny numbers at the level of round off errors.

Example 5. A 2D Euler system of equations without source terms

FE Jacobi, $\gamma=0.1$						
$N \times N$	L_1 error	L_1 order	L_∞ error	L_∞ order	iter#	CPU time
10×10	6.74E-04	-	2.68E-03	-	5817	12.92
20×20	1.30E-05	5.69	3.58E-05	6.23	6804	30.63
30×30	1.84E-06	4.83	4.76E-06	4.98	8583	68.08
40×40	4.49E-07	4.90	1.13E-06	5.00	10613	138.61
50×50	1.50E-07	4.92	3.74E-07	4.96	12725	247.23
60×60	6.08E-08	4.94	1.51E-07	4.95	14931	404.63
70×70	2.83E-08	4.95	7.04E-08	4.97	17068	616.05
80×80	1.46E-08	4.96	3.62E-08	4.99	19093	886.75
RK Jacobi, $\gamma=1.0$						
$N \times N$	L_1 error	L_1 order	L_∞ error	L_∞ order	iter#	CPU time
10×10	7.41E-04	-	2.68E-03	-	1746	4.16
20×20	1.31E-05	5.82	3.58E-05	6.23	2037	11.06
30×30	1.85E-06	4.84	4.76E-06	4.98	2568	26.47
40×40	4.51E-07	4.91	1.13E-06	5.00	3174	52.63
50×50	1.50E-07	4.93	3.74E-07	4.96	3825	94.11
60×60	6.10E-08	4.95	1.51E-07	4.95	4488	155.11
70×70	2.84E-08	4.96	7.04E-08	4.97	5130	236.75
80×80	1.46E-08	4.96	3.62E-08	4.99	5739	340.70
FE fast sweeping, $\gamma=1.0$						
$N \times N$	L_1 error	L_1 order	L_∞ error	L_∞ order	iter#	CPU time
10×10	6.62E-04	-	2.68E-03	-	560	1.26
20×20	1.30E-05	5.67	3.58E-05	6.23	653	4.02
30×30	1.84E-06	4.83	4.76E-06	4.98	821	10.69
40×40	4.49E-07	4.90	1.13E-06	5.00	1010	22.53
50×50	1.50E-07	4.92	3.74E-07	4.96	1213	42.39
60×60	6.08E-07	4.94	1.51E-07	4.95	1421	71.19
70×70	2.83E-08	4.95	7.04E-08	4.97	1622	110.55
80×80	1.46E-08	4.96	3.62E-08	4.99	1814	160.91

Table 4: Example 4, A 2D Euler system of equations with source terms. Accuracy, iteration numbers and CPU times of three different iterative schemes. CPU time unit: second

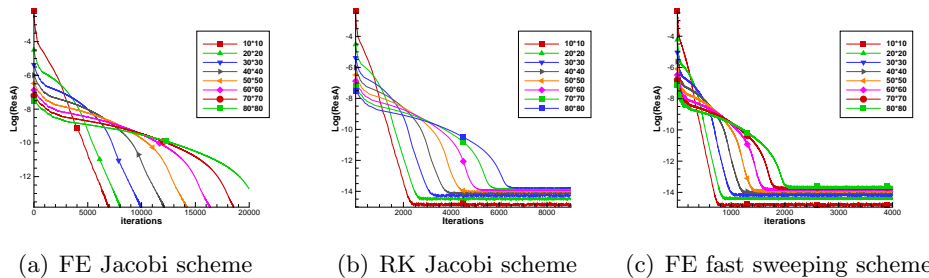


Figure 1: Example 4, A 2D Euler system of equations with source terms. The convergence history of the residue as a function of number of iterations for three schemes on different meshes.

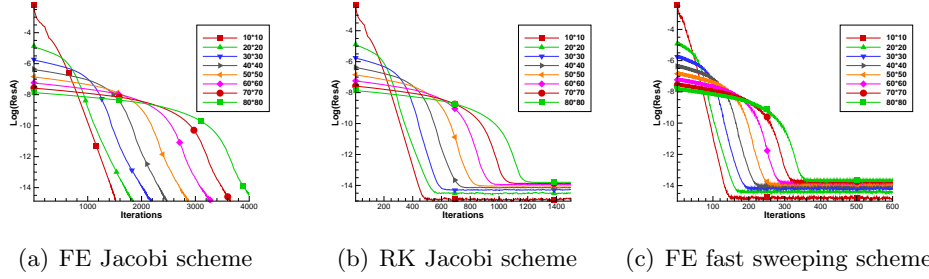


Figure 2: Example 5, A 2D Euler system of equations without source terms. The convergence history of the residue as a function of number of iterations for three schemes on different meshes.

In this example, we consider the following two-dimensional Euler system of equations

$$\frac{\partial}{\partial t} \begin{pmatrix} \rho \\ \rho u \\ \rho v \\ E \end{pmatrix} + \frac{\partial}{\partial x} \begin{pmatrix} \rho u \\ \rho u^2 + p \\ \rho uv \\ u(E + p) \end{pmatrix} + \frac{\partial}{\partial y} \begin{pmatrix} \rho v \\ \rho uv \\ \rho v^2 + p \\ v(E + p) \end{pmatrix} = 0$$

with the exact steady-state solutions $\rho(x, y, \infty) = 1 + 0.2 \sin(x - y)$, $u(x, y, \infty) = 1$, $v(x, y, \infty) = 1$, and $p(x, y, \infty) = 1$. The computational domain is $(x, y) \in [0, 2\pi] \times [0, 2\pi]$. Similar as the last example, we apply the exact steady-state solutions on the domain boundaries, and take the numerical initial conditions to be the same as the exact steady-state solutions in the iterative schemes. In Table 5, we show the numerical accuracy for the density variable ρ , iteration numbers and CPU times when these three different iterative schemes reach the average residue threshold value 10^{-12} of the convergence criterion. Similar conclusions can be drawn as the last example. All schemes have similar numerical errors and the fifth order accuracy when the iterations converge. However, The FE Jacobi scheme has to use a very small CFL number to reach convergence, which leads to large number of iterations and the most CPU time cost on refined meshes among all three schemes. Again, the FE fast sweeping scheme is the most efficient one among them, and it only takes about 40% CPU time costs of that of the RK Jacobi (TVD RK3) scheme. In Figure 2, the convergence history of the residue (3.1) as a function of number of iterations for these three schemes on different meshes is shown. It is verified that the residue of iterations settles down to tiny numbers at the level of round off errors for all three schemes.

3.2 Examples with non-smooth solutions

In this section, We test these schemes using problems with discontinuous solutions.

Example 6. One-dimensional steady shock

In this example we consider a 1D steady shock problem ([24, 26, 27])

$$U_t + F(U)_x = 0,$$

where $U = (\rho, \rho u, e)^T$, $F(U) = (\rho u, \rho u^2 + p, u(e + p))^T$. Here ρ, u, e are the density, velocity, and total energy respectively. p is the pressure and it is related to the total energy by $e = \frac{p}{\gamma' - 1} + \frac{1}{2} \rho u^2$, $\gamma' = 1.4$ which is the ratio of specific heat. The problem is defined on the domain $x \in [-1, 1]$. Initially the flow Mach number at the left of the shock wave is $M_\infty = 2$ with the shock wave located at $x = 0$. Periodic boundary conditions are applied here. The initial condition to start the

FE Jacobi, $\gamma=0.1$						
N×N	L ₁ error	L ₁ order	L _∞ error	L _∞ order	iter‡	CPU time
10×10	1.68E-03	-	8.01E-03	-	1233	1.11
20×20	2.38E-05	6.14	1.39E-04	5.85	1393	4.28
30×30	3.38E-06	4.82	1.93E-05	4.86	1684	10.97
40×40	8.29E-07	4.88	4.58E-06	5.00	2033	22.89
50×50	2.77E-07	4.91	1.52E-06	4.94	2410	42.27
60×60	1.13E-07	4.93	6.14E-07	4.97	2803	69.78
70×70	5.27E-08	4.94	2.85E-07	4.98	3219	108.63
80×80	2.72E-08	4.95	1.46E-07	4.98	3628	158.42
RK Jacobi, $\gamma=1.0$						
N×N	L ₁ error	L ₁ order	L _∞ error	L _∞ order	iter‡	CPU time
10×10	1.85E-03	-	8.01E-03	-	378	1.17
20×20	2.45E-05	6.24	1.39E-04	5.85	426	2.43
30×30	3.44E-06	4.84	1.93E-05	4.86	504	5.12
40×40	8.40E-07	4.90	4.58E-06	5.00	618	10.06
50×50	2.80E-07	4.92	1.52E-06	4.94	729	18.28
60×60	1.14E-07	4.94	6.14E-07	4.97	852	29.06
70×70	5.30E-08	4.95	2.85E-07	4.98	972	44.78
80×80	2.74E-08	4.96	1.46E-07	4.98	1095	64.31
FE fast sweeping, $\gamma=1.0$						
N×N	L ₁ error	L ₁ order	L _∞ error	L _∞ order	iter‡	CPU time
10×10	1.65E-03	-	8.01E-03	-	112	0.14
20×20	2.37E-05	6.12	1.39E-04	5.85	130	0.66
30×30	3.37E-06	4.81	1.93E-05	4.86	155	1.78
40×40	8.28E-07	4.88	4.58E-06	5.00	186	3.84
50×50	2.77E-07	4.91	1.52E-06	4.94	220	7.17
60×60	1.13E-07	4.93	6.14E-07	4.97	254	11.98
70×70	5.26E-08	4.94	2.85E-07	4.98	290	18.72
80×80	2.72E-08	4.95	1.46E-07	4.98	327	28.27

Table 5: Example 5, A 2D Euler system of equations without source terms. Accuracy, iteration numbers and CPU times of three different iterative schemes. CPU time unit: second

iterations in the schemes is given by the Rankine-Hugoniot jump condition (see e.g. [20]) as the following:

$$U(x, 0) = \begin{cases} U_l, & \text{if } x < 0; \\ U_r, & \text{if } x > 0, \end{cases}$$

where

$$\begin{pmatrix} p_l \\ \rho_l \\ u_l \end{pmatrix} = \begin{pmatrix} \frac{1}{\gamma' M_\infty^2} \\ 1 \\ 1 \end{pmatrix}, \quad \begin{pmatrix} p_r \\ \rho_r \\ u_r \end{pmatrix} = \begin{pmatrix} p_l \frac{2\gamma' M_\infty^2 - (\gamma' - 1)}{\gamma' + 1} \\ \frac{\gamma' + 1}{\gamma' - 1} \frac{p_r}{p_l} + 1 \\ \rho_l \frac{\gamma' + 1 + \frac{p_r}{p_l}}{\gamma' - 1} \\ \sqrt{\gamma' \frac{(2 + (\gamma' - 1) M_\infty^2) p_r}{(2\gamma' M_\infty^2 + (1 - \gamma')) \rho_r}} \end{pmatrix}.$$

In this example the initial condition is the same as the exact solution of the steady state. Similar as the previous examples, because the exact steady state solution of the PDE does not satisfy the numerical schemes, we will be able to see the convergence behavior that the iterative schemes drive the initial condition to the numerical steady states.

In this example, 400 uniformly spaced mesh points are used in the spatial discretization. In Table 6, we report number of iterations required to achieve convergence (i.e. to reach the convergence threshold value 10^{-12}), the final time and total CPU time when convergence is obtained for these three iterative schemes with different CFL numbers γ . The FE Jacobi iterative scheme requires a very small CFL number γ to converge. In this example, numerical tests show that γ needs to be less than or equal to 0.09. If $\gamma = 0.1$, the residue hangs at $10^{-10.9}$ and does not decrease till the pre-set maximum iteration number 100,000 is reached. The RK Jacobi scheme converges with much larger CFL numbers. Here, if γ is less than or equal to 1.2, the convergence criterion $ResA < 10^{-12}$ can be satisfied. If γ is increased to 1.3, the residue stops decreasing at $10^{-2.41}$. The FE fast sweeping method converges with similar CFL numbers as the RK Jacobi scheme. Here when γ is less than or equal to 1.1, the FE fast sweeping scheme converges. However, the FE fast sweeping method can converge to reach the residue threshold value 10^{-12} with much less iteration numbers and CPU times than the RK Jacobi scheme. In this example, with the smallest iteration numbers that each method can achieve to reach the convergence, the FE fast sweeping method has the CPU time cost 4.42 seconds while the RK Jacobi scheme needs 7.28 seconds, hence about 40% CPU time can be saved. In Figure 3, the convergence history of the residue (3.1) as a function of number of iterations for the RK Jacobi scheme and the FE fast sweeping scheme with different CFL numbers is shown. Again, we see that the residue of iterations settles down to tiny numbers at the level of round off errors.

In this one-dimensional problem whose steady state has shock wave, we draw the same conclusion as the previous examples with smooth solutions. The FE fast sweeping method is the most efficient approach for the fifth order multi-resolution WENO computations of the steady state problems among the three methods discussed in the paper, in terms of both iteration number and CPU time. This is further verified by the more complicated two dimensional simulations of Euler systems in the following examples.

Example 7. A two-dimensional oblique steady shock

In this example, we use these three iterative schemes to solve a two-dimensional oblique steady shock problem, which is a benchmark steady state problem (see e.g. [24, 26, 27]). The shock has an angle of 135° with the positive x-direction. The Mach number of the flow at the left of the shock is $M_\infty = 2$. The computational domain is $0 \leq x \leq 4$ and $0 \leq y \leq 2$. Initially the oblique shock wave passes the point (3, 0). The computational mesh has 200×100 equally spaced grid points with

FE Jacobi scheme			
γ : CFL number	iteration number	final time	CPU time
0.1	Not convergent	-	-
RK Jacobi scheme			
γ : CFL number	iteration number	final time	CPU time
0.1	80355	8.93	83.20
0.2	40515	9.00	43.17
0.4	20262	9.00	22.25
1.0	8118	9.02	8.97
1.1	7380	9.02	7.73
1.2	6765	9.02	7.28
1.3	Not convergent	-	-
FE fast sweeping scheme			
γ : CFL number	iteration number	final time	CPU time
0.1	26904	8.97	52.59
0.2	13164	8.77	25.66
0.4	5894	7.86	11.81
0.6	3776	7.55	7.81
1.0	2088	6.96	4.42
1.1	2426	8.89	4.50
1.2	Not convergent	-	-

Table 6: Example 6. 1D steady shock. Number of iterations, the final time and total CPU time when convergence is obtained. Convergence criterion threshold value is 10^{-12} . CPU time unit: second

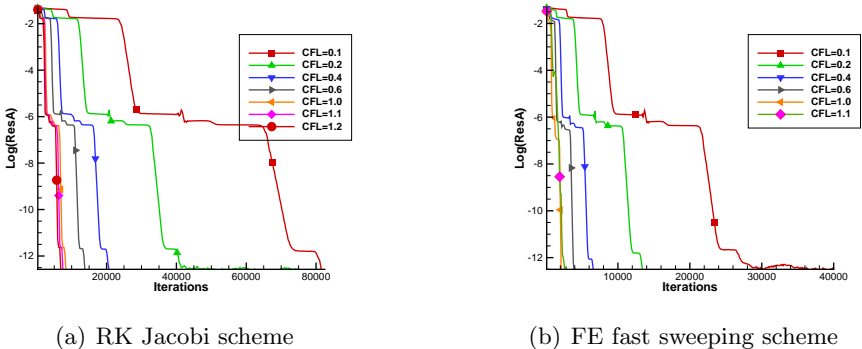


Figure 3: Example 6, One-dimensional steady shock. The convergence history of the residue as a function of number of iterations for two schemes with different CFL numbers.

FE Jacobi scheme			
γ : CFL number	iteration number	final time	CPU time
0.1	18391	17.25	2817.84
0.2	Not convergent	-	-
RK Jacobi scheme			
γ : CFL number	iteration number	final time	CPU time
0.3	19158	17.99	2895.34
0.4	14244	17.83	2151.48
0.5	11370	17.79	1718.41
0.6	Not convergent	-	-
FE fast sweeping scheme			
γ : CFL number	iteration number	final time	CPU time
0.3	6105	17.20	1668.17
0.4	4541	17.06	1244.56
0.5	3601	16.90	987.02
0.6	Not convergent	-	-

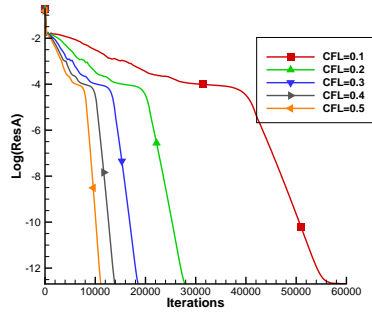
Table 7: Example 7. A two-dimensional oblique steady shock. Number of iterations, the final time and total CPU time when convergence is obtained. Convergence criterion threshold value is 10^{-12} . CPU time unit: second

$\Delta x = \Delta y$. Periodic boundary conditions are applied. The convergence criterion threshold value is set to be 10^{-12} .

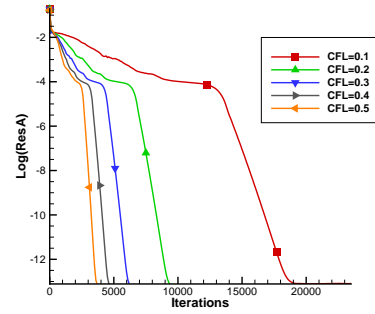
In Table 7, number of iterations required to reach the convergence threshold value 10^{-12} , the final time and total CPU time when convergence is obtained for these three iterative schemes with different CFL numbers γ are reported. As that in the 1D steady shock problem, the FE Jacobi scheme requires a very small CFL number $\gamma = 0.1$ to achieve the convergence, hence it needs a large amount of iteration numbers and CPU time. The RK Jacobi scheme relaxes the CFL number constraint and converges with much larger CFL numbers up to $\gamma = 0.5$, which reduces the CPU time from 2817.84 seconds of the FE Jacobi scheme to 1718.41 seconds. The FE fast sweeping method converges with similar CFL numbers as the RK Jacobi scheme, and it is more efficient than the RK Jacobi scheme with much reduced iteration numbers and CPU times. In fact, by using the largest possible CFL number to reach the convergence, the FE fast sweeping method only needs CPU time 987.02 seconds, which saves about 43% CPU time of the simulation by the TVD RK3 scheme (RK Jacobi). In Figure 4, residue history in terms of iterations for the RK Jacobi and the FE fast sweeping schemes with various CFL numbers is shown. We observe that the residue of iterations settles down to tiny numbers at the level of round off errors for both schemes. In Figure 5, contour plots of the density variable of the converged steady state solutions of the RK Jacobi and the FE fast sweeping schemes are shown, and it is verified that the similar results are obtained. In summary, we draw the consistent conclusion in this 2D steady shock wave example with that in the last 1D steady shock wave example, i.e., the FE fast Sweeping scheme is the most efficient one among these three iterative schemes.

Example 8. Regular shock reflection

In this example, we solve the two dimensional regular shock reflection problem by using the discussed iterative schemes. This problem is a typical and difficult benchmark problem of using high order schemes to simulate steady flow. As that found in [26, 27], even with advanced techniques to

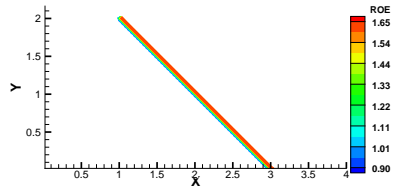


(a) RK Jacobi scheme

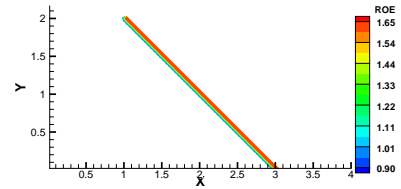


(b) FE fast sweeping scheme

Figure 4: Example 7, A two-dimensional oblique steady shock. The convergence history of the residue as a function of number of iterations for two schemes with different CFL numbers.



(a) RK Jacobi scheme



(b) FE fast sweeping scheme

Figure 5: Example 7, A two-dimensional oblique steady shock. 30 equally spaced density contours from 1.05 to 1.65 of the converged steady states of numerical solutions by two different iterative schemes.

improve the steady state convergence, it is still difficult for the residue of high order WENO schemes to converge to the level of round off errors. The fifth order fixed-point fast sweeping WENO scheme in [24] is also unable to drive the iteration residue to the level of round off errors. However, with the help of the unequal-sized sub-stencil WENO method such as the multi-resolution WENO scheme [37, 39], the absolutely convergent fixed-point fast sweeping method proposed here can make the iteration residue settle down to the round off error level easily, and at the same time maintain the high efficiency of the original fixed-point fast sweeping WENO scheme in [24]. This will be verified in the following numerical results.

Here the computational domain is a rectangle with the length 4 and the height 1. The boundary conditions in this problem consist of a reflection condition along the bottom boundary, supersonic outflow along the right boundary and Dirichlet conditions on the other two sides:

$$(\rho, u, v, p)^T = \begin{cases} (1.0, 2.9, 0, 5/7)^T |_{(0,y,t)^T}, \\ (1.69997, 2.61934, -0.50632, 1.52819)^T |_{(x,1,t)^T}. \end{cases}$$

The initial values at points in the entire domain are the same as those at the left boundary. The convergence criterion threshold value is set to be 10^{-12} . The computational grid is 120×30 .

In Table 8, number of iterations required to reach the convergence threshold value 10^{-12} , the final time and total CPU time when convergence is obtained for these three iterative schemes with different CFL numbers γ are reported. Again, the FE Jacobi scheme has to use a CFL number as small as $\gamma = 0.1$ in order to converge, which leads to many iterations and quite large CPU time cost. We find that the residue of the FE Jacobi scheme hangs at $10^{-11.8}$ if γ is increased to 0.2, and oscillate between $10^{-9.7}$ and $10^{-9.8}$ if $\gamma = 0.3$. By using the RK Jacobi (TVD RK3) scheme, the CFL number is enlarged to $\gamma = 0.6$ and the iterations converge much more efficiently than the FE Jacobi scheme. The FE fast sweeping scheme still turns out to be the most efficient one, which converges under the similar CFL numbers as the RK Jacobi scheme and only takes 98.92 seconds of CPU time to reach the steady state by using the largest possible CFL number. In fact, comparing to 289.89 seconds, the least CPU time cost case of the RK Jacobi scheme, the FE fast sweeping scheme saves about 66% CPU time cost to reach the steady state solution in this example. In Figure 6, residue history in terms of iterations for the RK Jacobi and the FE fast sweeping schemes with different CFL numbers is shown. We see that the residue of iterations settles down to values at the level of round off errors for all cases. This result justifies the performance improvement of the absolutely convergent fixed-point fast sweeping method proposed here over our previous work in [24]. In Figure 7, contour plots of the density variable of the converged steady state solutions of the RK Jacobi and the FE fast sweeping schemes are shown, and the similar results are obtained as expected.

FE Jacobi scheme			
γ : CFL number	iteration number	final time	CPU time
0.1	12046	5.09	618.36
0.2	Not convergent	-	-
RK Jacobi scheme			
γ : CFL number	iteration number	final time	CPU time
0.3	11268	4.76	579.22
0.4	8454	4.76	436.33
0.5	6762	4.76	348.09
0.6	5634	4.76	289.89
0.7	Not convergent	-	-
FE fast sweeping scheme			
γ : CFL number	iteration number	final time	CPU time
0.3	3651	4.62	188.14
0.4	2722	4.59	140.03
0.5	2170	4.57	111.91
0.6	1934	4.89	98.92
0.7	Not convergent	-	-

Table 8: Example 8, Regular shock reflection. Number of iterations, the final time and total CPU time when convergence is obtained. Convergence criterion threshold value is 10^{-12} . CPU time unit: second

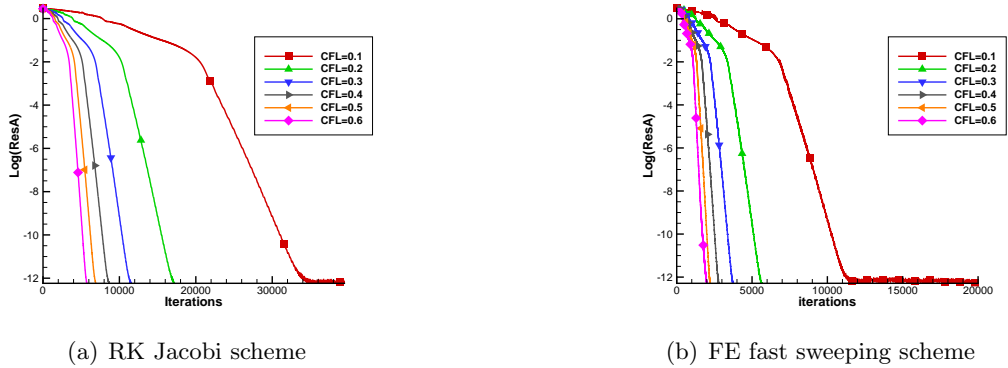


Figure 6: Example 8, Regular shock reflection. The convergence history of the residue as a function of number of iterations for two schemes with different CFL numbers.



Figure 7: Example 8, Regular shock reflection. 30 equally spaced density contours from 1.1 to 2.6 of the converged steady states of numerical solutions by two different iterative schemes.

Example 9. Supersonic flow past a plate with an attack angle

In the following we test the schemes by solving a series of benchmark problems about supersonic flow past two-dimensional plates from [36, 39]. The first example is a supersonic flow past a two-dimensional plate with an attack angle of $\alpha = 10^\circ$. The free stream Mach number is $M_\infty=3$. The ideal gas goes from the left toward the plate. The initial conditions are $p = \frac{1}{\gamma M_\infty^2}, \rho = 1, u = \cos(\alpha)$ and $v = \sin(\alpha)$. The computational domain is $[0, 10] \times [-5, 5]$. The plate is located at $x \in [1, 2]$ and $y = 0$. The slip boundary condition is imposed on the plate. The physical values of the inflow and outflow boundary conditions are applied in different directions. The computational grid is 200×200 . The convergence criterion threshold value is set to be 10^{-12} .

As that pointed out in [36, 39], for this kind of problems, although the boundary is very far away from the plate, the waves including the shocks and the rarefaction waves propagate to the far field boundaries. This makes it very challenging for the residue of high order schemes to converge to small values at the round off error level. Again, with the help of the multi-resolution WENO scheme [37], the iteration residue of the absolutely convergent fixed-point fast sweeping method proposed here settles down to the round off error level easily, and at the same time the high efficiency of the original fixed-point fast sweeping WENO scheme in [24] is preserved, as shown in the following numerical results.

In Table 9, number of iterations required to reach the convergence threshold value 10^{-12} , the final time and total CPU time when convergence is obtained for these three iterative schemes with different CFL numbers γ are reported. As previous examples, the FE Jacobi scheme has to use a CFL number as small as $\gamma = 0.1$ in order to converge, hence it takes a lot of CPU time cost. The RK Jacobi (TVD RK3) scheme increases the CFL number to $\gamma = 1.2$ and the iterations converge much more efficiently than the FE Jacobi scheme. In this example, the FE fast sweeping scheme can still converge with a larger CFL number ($\gamma = 1.4$) than the TVD RK3 scheme, and only takes 631.50 seconds of CPU time to reach the steady state by using the largest possible CFL number while the TVD RK3 scheme needs 1169.30 seconds of CPU time. 46% CPU time has been saved here. In Figure 8, residue history in terms of iterations for the RK Jacobi and the FE fast sweeping schemes with different CFL numbers is shown. It can be seen that the residue of iterations settles down to values at the level of round off errors for all cases. Again, this result verifies the performance improvement of the absolutely convergent fixed-point fast sweeping method proposed here over our previous work in [24]. In Figure 9, contour plots of the pressure variable of the converged steady state solutions of the RK Jacobi and the FE fast sweeping schemes are shown, and the comparable results are observed.

Example 10. Supersonic flow past two plates with an attack angle

In this example we replace one plate in Example 9 by two plates, i.e., a supersonic flow past two plates with an attack angle of $\alpha = 10^\circ$. The free stream Mach number is $M_\infty = 3$. The ideal gas goes from the left toward these two plates. The initial conditions are $p = \frac{1}{\gamma M_\infty^2}, \rho = 1, u = \cos(\alpha)$ and $v = \sin(\alpha)$. The computational domain is $[0, 10] \times [-5, 5]$. Two plates are placed at $x \in [2, 3]$ with $y = -2$ and at $x \in [2, 3]$ with $y = 2$. The slip boundary conditions are imposed on these plates. The physical values of the inflow and outflow boundary conditions are applied on all boundaries of the domain. The computational grid is 200×200 . The convergence criterion threshold value is set to be 10^{-12} .

The solution of this example contains strong shocks, rarefaction waves and their interactions. It is more complex than Example 9. Again, from the following numerical results, we can see that the iteration residue of the absolutely convergent fixed-point fast sweeping method proposed in this paper settles down to the round off error level easily, and it is the most efficient one among these three schemes discussed here.

FE Jacobi scheme			
γ : CFL number	iteration number	final time	CPU time
0.1	17337	30.53	4626.95
0.2	Not convergent	-	-
RK Jacobi scheme			
γ : CFL number	iteration number	final time	CPU time
0.4	13179	30.94	3527.08
0.5	10488	30.78	2811.88
0.7	7470	30.69	1994.08
1.0	5220	30.64	1406.23
1.2	4347	30.62	1169.30
1.3	Not convergent	-	-
FE fast sweeping scheme			
γ : CFL number	iteration number	final time	CPU time
0.4	3748	27.79	2043.47
0.5	2976	27.58	1622.19
0.7	2384	30.93	1294.97
0.9	1588	26.48	861.66
1.4	1164	29.87	631.50
1.5	Not convergent	-	-

Table 9: Example 9, supersonic flow past a plate with an attack angle. Number of iterations, the final time and total CPU time when convergence is obtained. Convergence criterion threshold value is 10^{-12} . CPU time unit: second

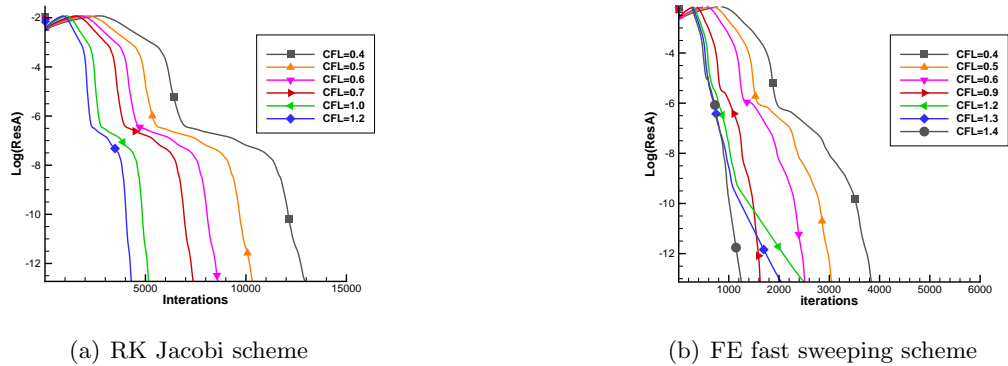


Figure 8: Example 9, supersonic flow past a plate with an attack angle. The convergence history of the residue as a function of number of iterations for two schemes with different CFL numbers.

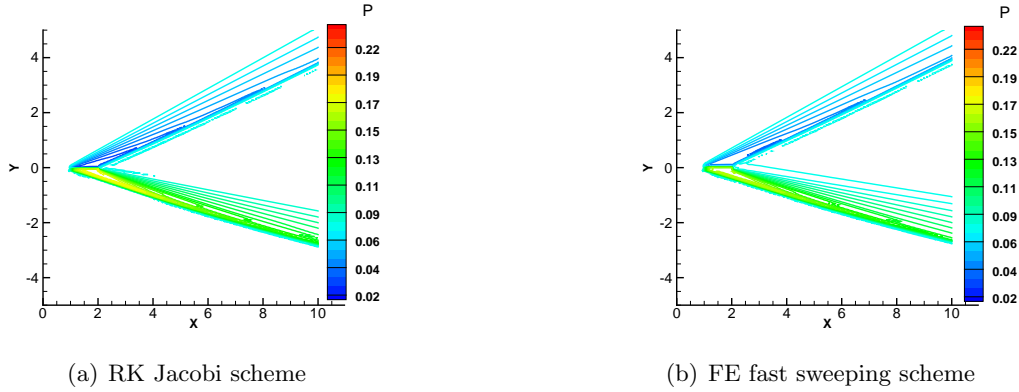


Figure 9: Example 9, supersonic flow past a plate with an attack angle. 30 equally spaced pressure contour from 0.02 to 0.23 of the converged steady states of numerical solutions by two different iterative schemes.

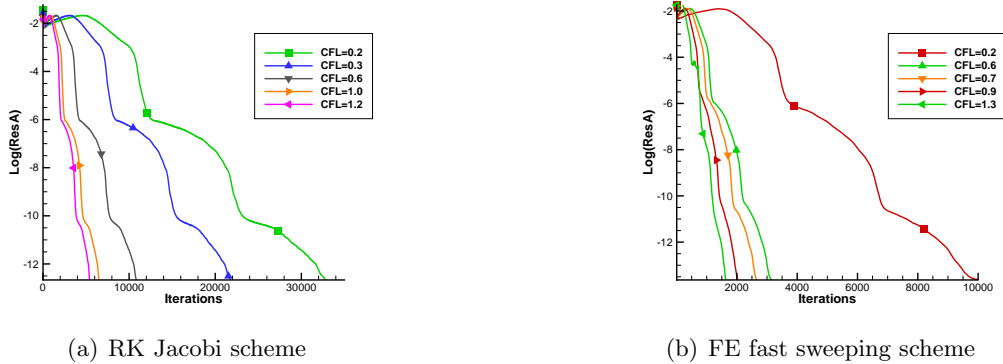


Figure 10: Example 10, supersonic flow past two plates with an attack angle. The convergence history of the residue as a function of number of iterations for two schemes with different CFL numbers.

In Table 10, number of iterations required to reach the convergence threshold value 10^{-12} , the final time and total CPU time when convergence is obtained for these three iterative schemes with different CFL numbers γ are reported. It is observed that the largest CFL number the FE Jacobi scheme can achieve for convergence is $\gamma = 0.1$ which makes it the most expensive one among these three schemes. The RK Jacobi (TVD RK3) scheme can use much larger CFL numbers till $\gamma = 1.2$, by which it only takes 1431.80 seconds of CPU time to reach the convergence threshold value. The FE fast sweeping scheme can use the largest CFL number $\gamma = 1.3$ to converge to the steady state solution in this example, which makes it the most efficient one. Only 810.30 seconds of CPU time are needed by the FE fast sweeping scheme to satisfy the convergence criterion, which saves more than 43% CPU time of that by the TVD RK3 scheme. In Figure 10, residue history in terms of iterations for the RK Jacobi and the FE fast sweeping schemes with different CFL numbers is shown. We see that the residue of iterations settles down to values at the level of round off errors for these cases. In Figure 11, contour plots of the pressure variable of the converged steady state solutions of the RK Jacobi and the FE fast sweeping schemes are presented, which show the comparable results.

FE Jacobi scheme			
γ : CFL number	iteration number	final time	CPU time
0.1	21316	37.53	5764.19
0.2	Not convergent	-	-
RK Jacobi scheme			
γ : CFL number	iteration number	final time	CPU time
0.3	21072	37.10	5701.58
0.6	10524	37.06	2863.86
1.0	6315	37.06	1716.80
1.2	5262	37.06	1431.80
1.3	Not convergent	-	-
FE fast sweeping scheme			
γ : CFL number	iteration number	final time	CPU time
0.6	2836	31.43	1535.53
0.7	2388	30.88	1303.16
0.8	2056	30.38	1125.40
0.9	1820	30.25	984.02
1.3	1476	35.23	810.30
1.4	Not convergent	-	-

Table 10: Example 10, supersonic flow past two plates with an attack angle. Number of iterations, the final time and total CPU time when convergence is obtained. Convergence criterion threshold value is 10^{-12} . CPU time unit: second

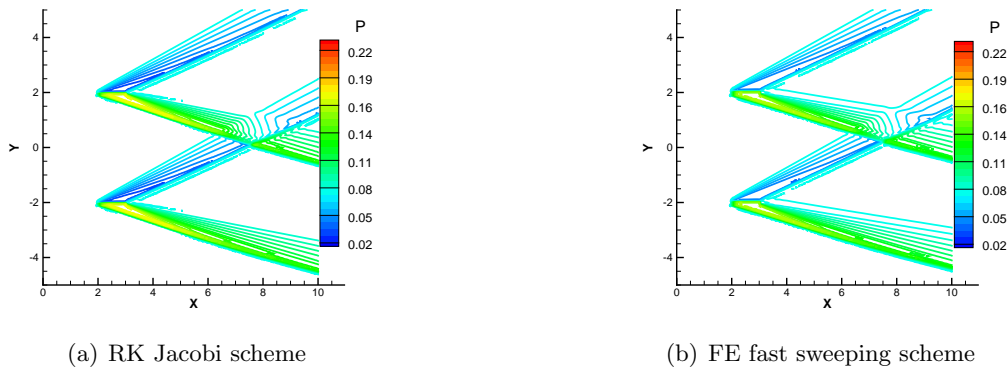


Figure 11: Example 10, supersonic flow past two plates with an attack angle. 30 equally spaced pressure contour from 0.02 to 0.23 of the converged steady states of numerical solutions by two different iterative schemes.

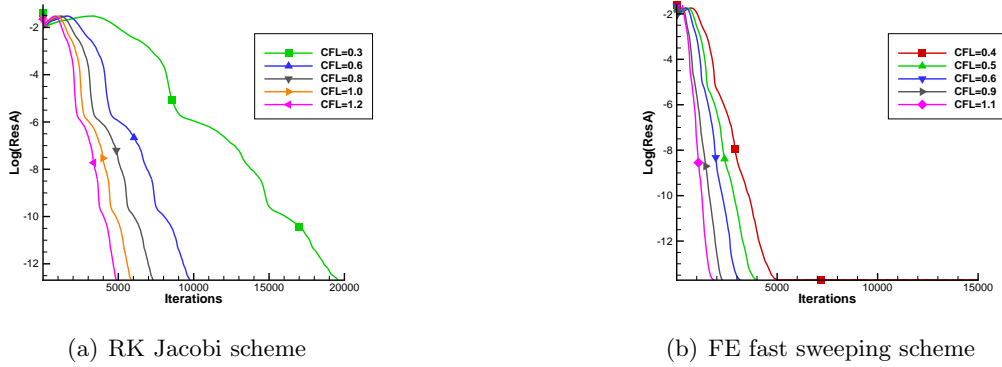


Figure 12: Example 11, supersonic flow past three plates with an attack angle. The convergence history of the residue as a function of number of iterations for two schemes with different CFL numbers.

Example 11. Supersonic flow past three plates with an attack angle

In this example we place three plates in the field such that there are more interactions of different waves and the flow is more complex than previous examples. The supersonic flow passes three plates with an attack angle of $\alpha = 10^\circ$. The free stream Mach number is $M_\infty = 3$. The ideal gas goes from the left side of the domain toward the plates. The initial conditions are $p = \frac{1}{\gamma' M_\infty^2}$, $\rho = 1$, $u = \cos(\alpha)$ and $v = \sin(\alpha)$. The computational domain is $[0, 10] \times [-5, 5]$. Three plates are placed at $x \in [2, 3]$ with $y = -2$, $x \in [1, 2]$ with $y = 0$, and $x \in [2, 3]$ with $y = 2$. We impose the slip boundary condition on these plates, and apply the physical values of the inflow and outflow boundary conditions on all boundaries of the computational domain. The computational grid is 200×200 . The convergence criterion threshold value is set to be 10^{-12} .

In Table 11, number of iterations required to reach the convergence threshold value 10^{-12} , the final time and total CPU time when convergence is obtained for these three iterative schemes with different CFL numbers γ are reported. Residue history in terms of iterations for the RK Jacobi and the FE fast sweeping schemes with different CFL numbers is shown in Figure 12, and contour plots of the pressure variable of the converged steady state solutions of the RK Jacobi and the FE fast sweeping schemes are presented in Figure 13. Based on these results for this more complex example, we draw similar conclusions as in previous examples. The proposed absolutely convergent fixed-point fast sweeping method is the most efficient scheme among all three schemes studied here. By using the largest CFL number permitted by each method to converge to steady states, the absolutely convergent fixed-point fast sweeping method saves about 40% CPU time of that by the TVD RK3 (RK Jacobi) scheme, while numerical steady states obtained by different schemes are comparable.

Example 12. Supersonic flow past a long plate with an attack angle

In this example, we test the schemes by solving the case of a long plate in the flow field, i.e., a supersonic flow past a long plate with an attack angle of $\alpha = 10^\circ$. The free stream has the Mach number $M_\infty = 3$. The ideal gas goes from the left toward the long plate. The initial condition to start the iterations is $p = \frac{1}{\gamma' M_\infty^2}$, $\rho = 1$, $u = \cos(\alpha)$ and $v = \sin(\alpha)$. The computational domain is $[0, 7] \times [-5, 5]$, and the long plate is set in the region $x \in [2, 7]$ with $y = 0$. The slip boundary condition is imposed on the long plate. The physical values of the inflow and outflow boundary conditions are applied at the boundaries of the computational domain. The difference from previous

FE Jacobi scheme			
γ : CFL number	iteration number	final time	CPU time
0.1	19235	33.88	5230.52
0.2	Not convergent	-	-
RK Jacobi scheme			
γ : CFL number	iteration number	final time	CPU time
0.3	18636	32.83	5056.52
0.6	9315	32.82	2536.50
1.0	5589	32.82	1520.80
1.2	4656	32.81	1267.42
1.3	Not convergent	-	-
FE fast sweeping scheme			
γ : CFL number	iteration number	final time	CPU time
0.5	3292	30.42	1802.92
0.6	2652	29.41	1448.73
0.8	1980	29.27	1079.00
0.9	1916	31.87	1050.42
1.1	1432	28.90	781.05
1.2	Not convergent	-	-

Table 11: Example 11, supersonic flow past three plates with an attack angle. Number of iterations, the final time and total CPU time when convergence is obtained. Convergence criterion threshold value is 10^{-12} . CPU time unit: second

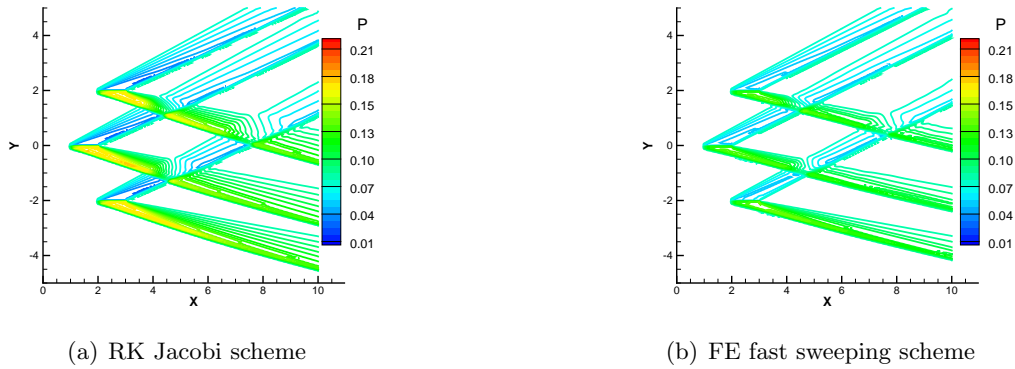


Figure 13: Example 11, supersonic flow past three plates with an attack angle. 30 equally spaced pressure contour from 0.01 to 0.22 of the converged steady states of numerical solutions by two different iterative schemes.

FE Jacobi scheme			
γ : CFL number	iteration number	final time	CPU time
0.1	36330	21.09	2630.02
0.2	Not convergent	-	-
RK Jacobi scheme			
γ : CFL number	iteration number	final time	CPU time
1.0	3702	22.76	731.28
1.2	3078	22.70	603.77
1.3	2838	22.67	556.39
1.4	2637	22.68	518.45
1.5	Not convergent	-	-
FE fast sweeping scheme			
γ : CFL number	iteration number	final time	CPU time
1.0	1048	19.27	396.86
1.2	846	19.04	328.58
1.3	788	18.78	297.14
1.4	Not convergent	-	-

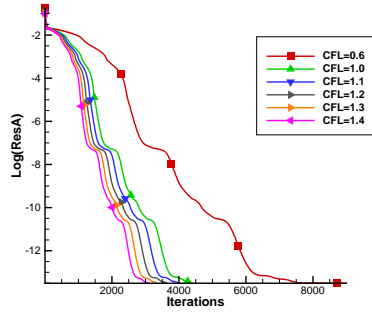
Table 12: Example 12, supersonic flow past a long plate with an attack angle. Number of iterations, the final time and total CPU time when convergence is obtained. Convergence criterion threshold value is 10^{-13} . CPU time unit: second

examples is that the plate extends to the right boundary, so the shock waves and the rarefaction waves pass through the right boundary on both sides of the plate. The computational grid is 140×200 . The convergence criterion threshold value is set to be 10^{-13} .

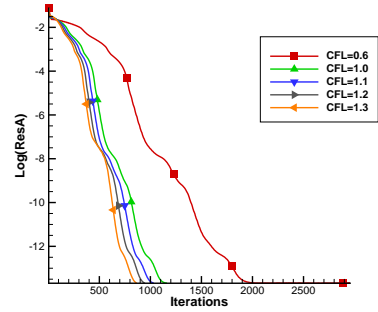
In Table 12, number of iterations required to reach the convergence threshold value 10^{-13} , the final time and total CPU time when convergence is obtained for these three iterative schemes with different CFL numbers γ are reported. Residue history in terms of iterations for the RK Jacobi and the FE fast sweeping schemes with different CFL numbers is shown in Figure 14, and contour plots of the pressure variable of the converged steady state solutions of the RK Jacobi and the FE fast sweeping schemes are presented in Figure 15. Again, we observe that the absolutely convergent fixed-point fast sweeping method (FE fast sweeping scheme) is the most efficient scheme among all three schemes studied here. By using the largest CFL number permitted by each method to converge to steady states, the absolutely convergent fixed-point fast sweeping method saves about 43% CPU time of that by the TVD RK3 (RK Jacobi) scheme, while numerical steady states obtained by these schemes are comparable.

Example 13. Supersonic flow past three long plates

In the last example, we test the schemes by solving the case of a supersonic flow past three long plates with an attack angle of $\alpha = 10^\circ$. The free stream Mach number is still $M_\infty = 3$. The ideal gas goes from the left toward these three long plates. The initial condition to start the iterations is $p = \frac{1}{\gamma M_\infty^2}$, $\rho = 1$, $u = \cos(\alpha)$ and $v = \sin(\alpha)$. The computational field is $[0, 5] \times [-5, 5]$. The long plates are placed at $x \in [2, 5]$ with $y = -2$, $x \in [2, 5]$ with $y = 0$, and $x \in [2, 5]$ with $y = 2$. The slip boundary condition is imposed on these three long plates, and the physical values of the inflow and outflow boundary conditions are applied at the left, right, bottom, and top boundaries of the domain. In this example, the plates also extend to the right boundary as Example 12, however more plates than Example 12 lead to more complicated interactions of the shocks and the rarefaction

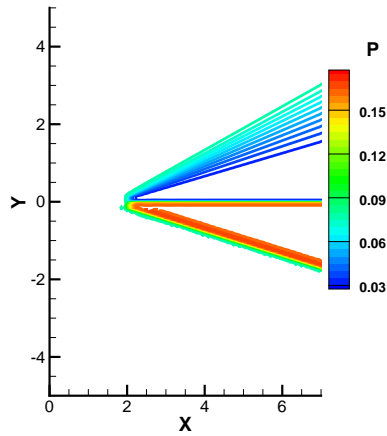


(a) RK Jacobi scheme

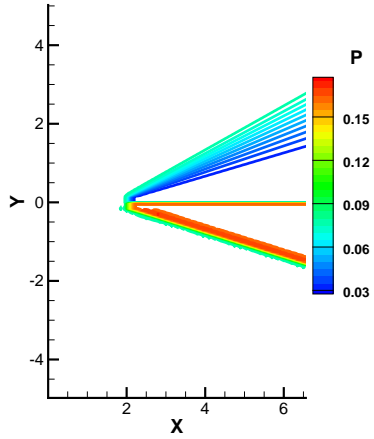


(b) FE fast sweeping scheme

Figure 14: Example 12, supersonic flow past a long plate with an attack angle. The convergence history of the residue as a function of number of iterations for two schemes with different CFL numbers.



(a) RK Jacobi scheme



(b) FE fast sweeping scheme

Figure 15: Example 12, supersonic flow past a long plate with an attack angle. 30 equally pressure contour from 0.03 to 0.17 of the converged steady states of numerical solutions by two different iterative schemes.

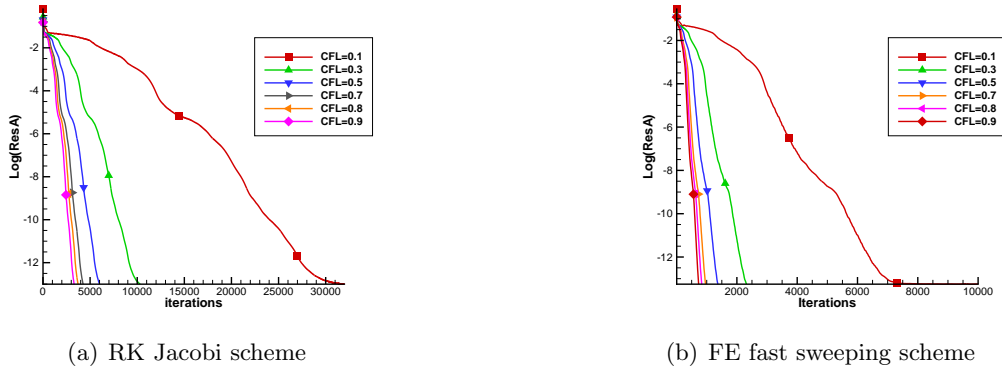


Figure 16: Example 13, supersonic flow past three long plates with an attack angle. The convergence history of the residue as a function of number of iterations for two schemes with different CFL numbers.

waves which pass through the right boundary on both sides of the plates. The computational grid is 100×200 . The convergence criterion threshold value is set to be 10^{-13} .

In Table 13, number of iterations required to reach the convergence threshold value 10^{-13} , the final time and total CPU time when convergence is obtained for these three iterative schemes with different CFL numbers γ are reported. Residue history in terms of iterations for the RK Jacobi and the FE fast sweeping schemes with different CFL numbers is presented in Figure 16, and contour plots of the pressure variable of the converged steady state solutions of the RK Jacobi and the FE fast sweeping schemes are shown in Figure 17. In this last example, we obtain the consistent conclusion with other examples, i.e., the proposed absolutely convergent fixed-point fast sweeping method (FE fast sweeping scheme) is the most efficient scheme among all three schemes studied here, in terms of both iteration numbers and CPU times to reach the convergence criterion. By using the largest CFL number permitted by each method to converge to steady states, the absolutely convergent fixed-point fast sweeping method saves more than 58% CPU time of that by the TVD RK3 (RK Jacobi) scheme, while numerical steady states obtained by these schemes are comparable.

4 Concluding remarks

In a recent work [24], the fast sweeping techniques were incorporated into a fifth order WENO method for efficiently solving steady state problems of hyperbolic conservation laws. It was found that by using the fast sweeping techniques, the forward Euler scheme with the fifth order WENO spatial discretization achieves a much larger CFL number than that in a regular time marching approach, hence it is much more efficient to converge to steady states of the high order WENO scheme. The forward Euler fast sweeping method is also more efficient than the popular TVD RK3 scheme to converge to steady states. However, an open problem in the fast sweeping WENO scheme in [24] is that for some benchmark numerical examples, the iteration residue hangs at a truncation error level instead of converging to machine zero / round off errors. In this paper, we adopt the fifth order multi-resolution WENO scheme in [37] and form a novel absolutely convergent forward Euler type fixed-point fast sweeping method for steady state of hyperbolic conservation laws. Extensive numerical experiments, including solving difficult problems which are challenging for high order schemes to converge to steady states, verify that the fast sweeping scheme can significantly enlarge

FE Jacobi scheme			
γ : CFL number	iteration number	final time	CPU time
0.1	10497	14.26	1481.52
0.2	Not convergent	-	-
RK Jacobi scheme			
γ : CFL number	iteration number	final time	CPU time
0.5	6003	13.59	851.97
0.7	4257	13.50	603.83
0.9	3303	13.46	469.42
1.0	Not convergent	-	-
FE fast sweeping scheme			
γ : CFL number	iteration number	final time	CPU time
0.5	1340	12.33	365.42
0.8	824	12.12	225.39
0.9	720	11.91	195.45
1.0	Not convergent	-	-

Table 13: Example 13, supersonic flow past three long plates with an attack angle. Number of iterations, the final time and total CPU time when convergence is obtained. Convergence criterion threshold value is 10^{-13} . CPU time unit: second

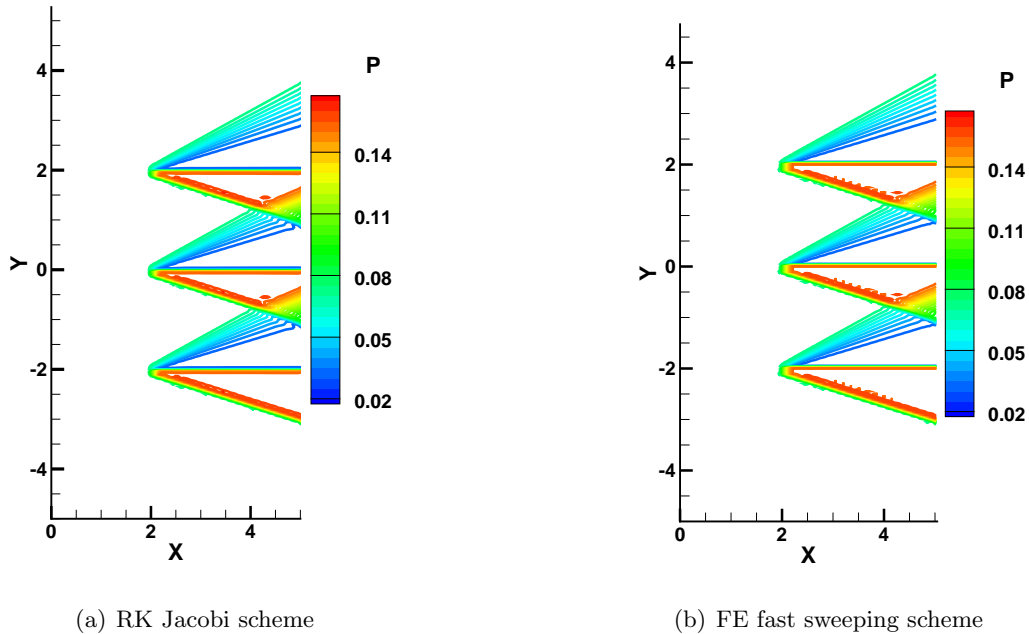


Figure 17: Example 13, supersonic flow past three long plates with an attack angle. 30 equally pressure contour from 0.02 to 0.17 of the converged steady states of numerical solutions by two different iterative schemes.

the CFL number of the forward Euler scheme with a high order WENO spatial discretization (e.g., a fifth order WENO scheme) to the level of the TVD RK3 scheme. Furthermore, more than 40% to 60% CPU time is saved by using the forward Euler type fixed-point fast sweeping method rather than the TVD RK3 scheme to converge to steady states of the WENO scheme. The residue of the new absolutely convergent fast sweeping iterations converges to machine zero / round off errors for all benchmark problems tested in this paper. In the future, we will extend the proposed scheme to that on unstructured meshes for solving steady state problems on complex domains.

References

- [1] R. Borges, M. Carmona, B. Costa and W.S. Don, *An improved weighted essentially non-oscillatory scheme for hyperbolic conservation laws*, J. Comput. Phys., 227 (2008), 3191-3211.
- [2] G. Capdeville, *A central WENO scheme for solving hyperbolic conservation laws on non-uniform meshes*, Journal of Computational Physics, 227 (2008), 2977-3014.
- [3] M. Castro, B. Costa and W.S. Don, *High order weighted essentially non-oscillatory WENO-Z schemes for hyperbolic conservation laws*, J. Comput. Phys., 230 (2011), 1766-1792.
- [4] S. Chen, *Fixed-point fast sweeping WENO methods for steady state solution of scalar hyperbolic conservation laws*, International Journal of Numerical Analysis and Modeling, 11 (2014), 117-130.
- [5] W. Chen, C.-S. Chou and C.-Y. Kao, *Lax-Friedrichs fast sweeping methods for steady state problems for hyperbolic conservation laws*, Journal of Computational Physics, 234 (2012), 452-471.
- [6] M. Dumbser and M. Käser, *Arbitrary high order non-oscillatory finite volume schemes on unstructured meshes for linear hyperbolic systems*, J. Comput. Phys., 221 (2007), 693-723.
- [7] S. Fomel, S. Luo and H. Zhao, *Fast sweeping method for the factored eikonal equation*, Journal of Computational Physics, 228 (2009), 6440-6455.
- [8] S. Gottlieb, C.-W. Shu and E. Tadmor, *Strong stability-preserving high-order time discretization methods*, SIAM Review, 43 (2001), 89-112.
- [9] W. Hao, J.D. Hauenstein, C.-W. Shu, A.J. Sommesse, Z. Xu and Y.-T. Zhang, *A homotopy method based on WENO schemes for solving steady state problems of hyperbolic conservation laws*, Journal of Computational Physics, 250, (2013), 332-346.
- [10] C. Hu and C.-W. Shu, *Weighted essentially non-oscillatory schemes on triangular meshes*, Journal of Computational Physics, 150 (1999), 97-127.
- [11] G.-S. Jiang and C.-W. Shu, *Efficient implementation of weighted ENO schemes*, Journal of Computational Physics, 126 (1996), 202-228.
- [12] D. Levy, S. Nayak, C.-W. Shu and Y.-T. Zhang, *Central WENO schemes for Hamilton-Jacobi equations on triangular meshes*, SIAM Journal on Scientific Computing, 28 (2006), 2229-2247.
- [13] D. Levy, G. Puppo and G. Russo, *Central WENO schemes for hyperbolic systems of conservation laws*, Mathematical Modelling and Numerical Analysis, 33 (1999), 547-571.

- [14] D. Levy, G. Puppo and G. Russo, *Compact central WENO schemes for multidimensional conservation laws*, SIAM J. Sci. Comput., 22 (2000), 656-672.
- [15] F. Li, C.-W. Shu, Y.-T. Zhang and H.-K. Zhao, *A second order discontinuous Galerkin fast sweeping method for Eikonal equations*, Journal of Computational Physics, 227 (2008), 8191-8208.
- [16] X.-D. Liu, S. Osher and T. Chan, *Weighted essentially non-oscillatory schemes*, Journal of Computational Physics, 115 (1994), 200-212.
- [17] Y. Liu and Y.-T. Zhang, *A robust reconstruction for unstructured WENO schemes*, Journal of Scientific Computing, 54 (2013), 603-621.
- [18] J. Qian, Y.-T. Zhang and H.-K. Zhao, *Fast sweeping methods for Eikonal equations on triangular meshes*, SIAM Journal on Numerical Analysis, 45 (2007), 83-107.
- [19] J. Qian, Y.-T. Zhang and H.-K. Zhao, *A fast sweeping method for static convex Hamilton-Jacobi equations*, Journal of Scientific Computing, 31 (2007), 237-271.
- [20] M.A. Saad, *Compressible Fluid Flow*. Prentice Hall, New York, (1993).
- [21] C.-W. Shu, *Essentially non-oscillatory and weighted essentially non-oscillatory schemes for hyperbolic conservation laws*, in *Advanced Numerical Approximation of Nonlinear Hyperbolic Equations*, B. Cockburn, C. Johnson, C.-W. Shu and E. Tadmor (Editor: A. Quarteroni), Lecture Notes in Mathematics, volume 1697, Springer, Berlin, 1998, 325-432.
- [22] C.-W. Shu and S. Osher, *Efficient implementation of essentially non-oscillatory shock capturing schemes*, Journal of Computational Physics, 77 (1988), 439-471.
- [23] L. Wu and Y.-T. Zhang, *A third order fast sweeping method with linear computational complexity for Eikonal equations*, Journal of Scientific Computing, 62 (2015), 198-229.
- [24] L. Wu, Y.-T. Zhang, S. Zhang and C.-W. Shu, *High order fixed-point sweeping WENO methods for steady state of hyperbolic conservation laws and its convergence study*, Communications in Computational Physics, 20 (2016), 835-869.
- [25] T. Xiong, M. Zhang, Y.-T. Zhang and C.-W. Shu, *Fast sweeping fifth order WENO scheme for static Hamilton-Jacobi equations with accurate boundary treatment*, Journal of Scientific Computing, 45 (2010), 514-536.
- [26] S. Zhang, S. Jiang and C.-W. Shu, *Improvement of convergence to steady state solutions of Euler equations with the WENO schemes*, Journal of Scientific Computing, 47 (2011), 216-238.
- [27] S. Zhang and C.-W. Shu, *A new smoothness indicator for the WENO schemes and its effect on the convergence to steady state solutions*, Journal of Scientific Computing, 31 (2007), 273-305.
- [28] Y.-T. Zhang, S. Chen, F. Li, H. Zhao and C.-W. Shu, *Uniformly accurate discontinuous Galerkin fast sweeping methods for Eikonal equations*, SIAM Journal on Scientific Computing, 33 (2011), 1873-1896.
- [29] Y.-T. Zhang and C.-W. Shu, *High order WENO schemes for Hamilton-Jacobi equations on triangular meshes*, SIAM Journal on Scientific Computing, 24 (2003), 1005-1030.

- [30] Y.-T. Zhang and C.-W. Shu, *Third order WENO schemes on three dimensional tetrahedral meshes*, Communications in Computational Physics, 5 (2009), 836-848.
- [31] Y.-T. Zhang, H.-K. Zhao and S. Chen, *Fixed-point iterative sweeping methods for static Hamilton-Jacobi equations*, Methods and Applications of Analysis, 13 (2006), 299-320.
- [32] Y.-T. Zhang, H.-K. Zhao and J. Qian, *High order fast sweeping methods for static Hamilton-Jacobi equations*, Journal of Scientific Computing, 29 (2006), 25-56.
- [33] H.-K. Zhao, *A fast sweeping method for Eikonal equations*, Math. Comp., 74 (2005), 603-627.
- [34] X. Zhong and C.-W. Shu, *A simple weighted essentially nonoscillatory limiter for Runge- Kutta discontinuous Galerkin methods*, J. Comput. Phys., 232 (2013), 397-415.
- [35] J. Zhu and J. Qiu, *A new type of finite volume WENO schemes for hyperbolic conservation laws*, Journal of Scientific Computing, 73 (2017), 1338-1359.
- [36] J. Zhu and C.-W. Shu, *Numerical study on the convergence to steady state solutions of a new class of high order WENO schemes*, Journal of Computational Physics, 349 (2017), 80-96.
- [37] J. Zhu and C.-W. Shu, *A new type of multi-resolution WENO schemes with increasingly higher order of accuracy*, Journal of Computational Physics, 375 (2018), 659-683.
- [38] J. Zhu and C.-W. Shu, *A new type of third-order finite volume multi-resolution WENO schemes on tetrahedral meshes*, Journal of Computational Physics, v406 (2020), 109212.
- [39] J. Zhu and C.-W. Shu, *Convergence to steady-state solutions of the new type of high-order multi-resolution WENO schemes: a numerical study*, Communications on Applied Mathematics and Computation, v2 (2020), 429-460.